ISSN 1068-1620, Russian Journal of Bioorganic Chemistry, 2022, Vol. 48, No. 3, pp. 467–490. © Pleiades Publishing, Ltd., 2022.
Russian Text © The Author(s), 2022, published in Bioorganicheskaya Khimiya, 2022, Vol. 48, No. 4, pp. 415–441.

REVIEW ARTICLE

Fluorescent Probes for HOCl Detection in Living Cells

V. E. Reut[a], I. V. Gorudko[a], D. V. Grigorieva[a], A. V. Sokolov[b, c, d], and O. M. Panasenko[d, 1]

[a] *Belarusian State University, Minsk, 220030 Belarus*
[b] *Institute of Experimental Medicine, St. Petersburg, 197376 Russia*
[c] *St. Petersburg State University, St. Petersburg, 199034 Russia*
[d] *Federal Research and Clinical Center of Physical-Chemical Medicine, Federal Medical Biological Agency, Moscow, 119435 Russia*

Received August 2, 2021; revised October 12, 2021; accepted November 22, 2021

Abstract—Hypochlorous acid (HOCl) plays an important role in the immune system not only protecting the organism from pathogens, but also, due to its high reactivity, provoking the development and complication of many diseases. Therefore, the development of highly sensitive and selective HOCl biosensors, including fluorescent probes, to better understand the roles of HOCl in living systems, is of great importance. Nevertheless, there are many difficulties associated with HOCl registration in biological probes (chemo- and photostability, cytotoxicity, fluorescence and absorption characteristics, selectivity, sensitivity, etc.). Thus, the development of new chemosensors has been relevant for many years. In this review, we describe classification of small-molecule probes for HOCl detection in biological systems, as well as summarize the results of the development of chemosensors, their photophysical properties, and biological applications. Particular attention is paid to the achievements in this area over the years 2016–2021. A number of problems related to the design and application of small-molecule probes are formulated. Due to the absence of a "gold standard" among the HOCl chemosensors, which is associated with the commercial unavailability or complex methods of synthesis of new sensors as well, some recommendations are given regarding the field of the chemosensor application. Trends in the development of fluorescent chemosensors for HOCl visualization in living cells are outlined.

Keywords: fluorescence, fluorescent probes, reactive oxygen species, reactive halogen species, hypochlorous acid, chemosensors

DOI: 10.1134/S1068162022030165

Contents

Abbreviations: DAMN, diaminomaleonitrile; ESIPT, excited state intramolecular proton transfer; FRET, Forster resonance energy transfer; HeLa, human cervical cancer cell line; HL-60, human acute promyelocyte leukosis cell line; ICT, intramolecular charge transfer; IFN-γ, interferon gamma; LPS, lipopolysaccharides; MPO, myeloperoxidase; PET, photoinduced electron transfer; PMA, phorbol 12-myristate 13-acetate; R-19, rhodamine 19; RAW264.7, murine virus-transformed macrophage-like cell line; TBET, through bond energy transfer; RNS, reactive nitrogen species; RHS, reactive halogen species; ROS, reactive oxygen species; em, emission; ex, excitation; LOD, limit of detection; APF, aminophenyl fluorescein; CB, celestine blue B; Hcy, homocysteine; RGNH, rhodamine 6G naphthoyl hydrazide; SNAPF, sulfonaphthoaminophenyl fluorescein.

[1] Corresponding author: phone: +7 (499) 246-44-90; e-mail: o-panas@mail.ru.

INTRODUCTION

Reactive oxygen (ROS), nitrogen (RNS), and halogen species (RHS) produced by living organisms, are necessary for various biological functions: intercellular interaction, intracellular signaling, modulation of blood pressure, control of the immune system, phagocytosis, regulation of the activity of enzymes and transcription factors, synthesis of biological compounds, metabolic processes, etc. [1, 2]. However, due to their high reactivity, these compounds, while modifying biologically important molecules (nucleic acids, proteins, lipids, etc.), are also involved in pathological processes, such as aging, diabetes, neurodegenerative and cardiovascular diseases, cancer, cataracts, rheumatoid arthritis, inflammation, ischemic, and postischemic pathologies [3]. Among RHS, hypochlorous acid (HOCl), produced by myeloperoxidase (MPO, EC 1.11.2.2), an enzyme found mainly in azurophilic granules of neutrophils and to a lesser extent in monocytes, is involved in both peroxidase and chlorination reactions and plays a special role in protection of the body from external pathogens [4, 5]. The pK_a value of HOCl is 7.5; at physiological pH, almost equal concentrations of HOCl and OCl^- are present in water; therefore, hereinafter, HOCl is understood as a mixture of these forms ($HOCl/OCl^-$) [6]. An increase in the concentration of MPO in the blood plasma and excessive formation of HOCl and chlorinated products result in damage to the host cells and tissues. Many inflammatory diseases (atherosclerosis, cardiovascular, neurodegenerative diseases, vasculitis, fibrosis, rheumatoid arthritis, some types of cancer, etc.) are accompanied by an increase in the amount and/or activity of MPO, an increase in HOCl production and, as a result, detection of the so-called markers of halogenative stress (3-chlorotyrosine, 5-chlorouracil, α-chloroaldehydes, chlorinated proteins, etc.) in biological fluids of patients with these pathologies [6, 7]. In view of the exceptional role of HOCl in both protecting the body from pathogens and development of pathologies, studies on the kinetics of HOCl formation, its localization, ways of regulating MPO activity, and identification of the contribution of MPO to the development of diseases, make up important fundamental and applied problems aimed at prevention, diagnosis, and monitoring of the treatment of the diseases associated with inflammation.

Detection of HOCl is associated with a number of difficulties. HOCl is highly reactive and has a short lifetime in biological media. Thus, the rate constants of the reactions of HOCl with cysteine and methionine exceed 10^7 M^{-1} s^{-1}, while with histidine, taurine, and α-amino groups it exceed 10^5 M^{-1} s^{-1} [8]. Reactions with other targets are also possible (with NH_2 groups of "polar heads" of phosphatidylethanolamine and phosphatidylserine; DNA; with addition to double bond and to aromatic rings in proteins and lipids), but they are unlikely to play a decisive role due to lower reaction rates. Moreover, phagocytes also generate a number of other highly reactive compounds: ROS ($^{\bullet}O_2^-$, H_2O_2, $^1O_2$, $^{\bullet}OH$, $ROO^{\bullet}$, etc.), RNS ($^{\bullet}NO$, $ONOO^-$, NO_2^-, $^{\bullet}NO_2$, etc.), as well as RHS (in addition to HOCl, HOBr, chloramines, bromamines, etc. can be formed) [3, 9]. Considering all this, reliable, sensitive, and selective detection tools with high spatial and temporal resolution are needed to detect HOCl production in biological systems. Fluorescence analysis based on synthetic probes (chemosensors) is this powerful tool that combines ease of manipulation and availability [10, 11]. Despite the fact that in recent years many chemosensors have been developed that can detect HOCl and other ROS, RHS, and RNS, such disadvantages as low stability, lack of specificity of their reactions with oxidizing agents, or the strong influence of reducing agents, as well as cytotoxicity, make the search for new fluorescent probes capable of registering HOCl in biological systems a topical problem.

Most of the experimental studies and analytical reviews devoted to this topic are focused on physicochemical aspects of the interaction of probes with HOCl in a cell-free medium, as well as the prospects for the development of new probes [10–14]. Less attention has been given to the use of these probes for detecting HOCl in cellular media. In view of the fact that the ultimate goal of sensor development is to study the contribution of HOCl to physiological and pathophysiological processes, screening of drugs, and prediction and diagnosis of diseases, it is extremely important to study the possibility of using these substances in cell/tissue/organism systems. This review contains information on the most promising small-molecule fluorescent probes designed to detect HOCl in cellular systems. We also note that some issues related to the use of nanoparticles and quantum dots for detecting HOCl are presented in [15–17] and will not be discussed in this review.

TYPES OF MOLECULAR FLUORESCENCE PROBES FOR HOCl REGISTRATION

The choice of a fluorescent probe depends on the objectives of the study. Meanwhile, sensitivity and selectivity of the probe with respect to the analyte (the substance the content of which is to be estimated; in our case, HOCl) are often the determining factors in choosing a sensor. Limit of detection (LOD) is most often used as a quantitative measure of probe sensitivity to HOCl [18]. The mathematical expression used for calculating the LOD looks like this:

$$LOD = 3\sigma/k,$$

where σ is the standard deviation of the fluorescence intensity of the probe solution in the absence of HOCl and k is the slope of the calibration curve of the dependence of the fluorescence intensity on the HOCl concentration [19]. Selectivity is understood as preferred

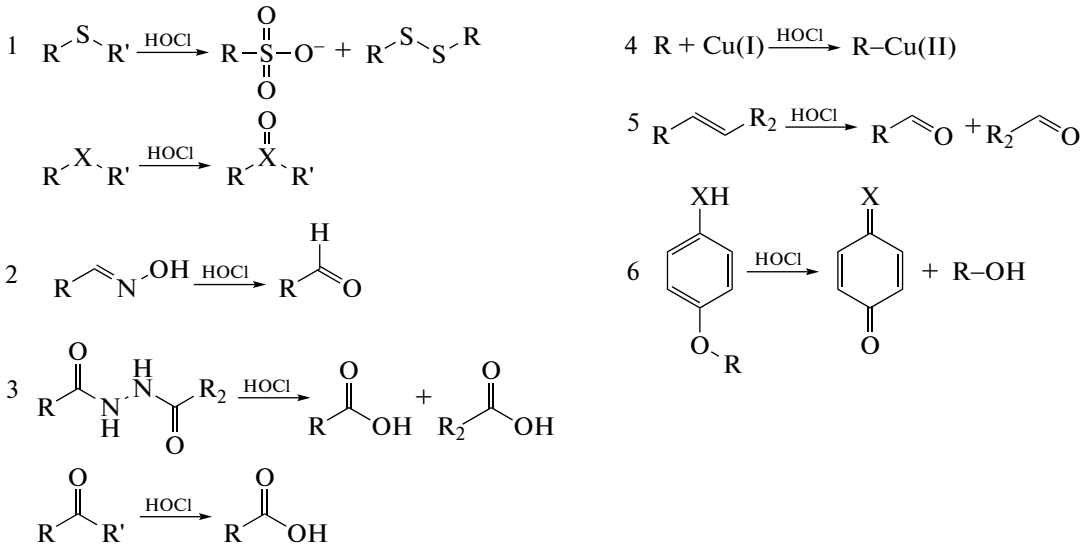

Fig. 1. Interactions between chemosensors and HOCl (R is a fluorophore). HOCl reaction: (1) with X-containing compounds (X = S, Se, Te; R' = H or alkyl); (2) with oxime derivatives; (3) with hydrazines and amides (R' = NH_2); (4) with Cu(I)-containing compounds; (5) with an unsaturated carbon–carbon bond; (6) with derivatives of *p*-methoxyphenol (X = O) and *p*-aminophenol (X = NR', R' = H or alkyl). Adapted from [16, 22].

interaction of the probe with HOCl compared to other compounds. Most often, in experimental articles, a probe is recognized as sensitive if the change in its fluorescence intensity under the action of HOCl is significantly greater than under the action of other highly reactive compounds present. Sensitivity and selectivity of a probe can be limited by both the chemical conversion mechanism of the sensor and type of conversion of the fluorescent response or use of particular fluorophores.

Classification of Probes according to the Reaction Site

The development of fluorescent probes for detecting HOCl is based on redox or substitution reactions between HOCl and the chemosensor. Examples of some of the main reactions of HOCl with functional groups of fluorescent probes are shown in Fig. 1:

(1) Sulfur-containing compounds are oxidized under the influence of HOCl with the formation of sulfonates, disulfides, or sulfoxides; selenium- and tellurium-containing compounds, to selenium- and tellurium oxides, respectively (Fig. 1, 1) [20].

(2) Oxime derivatives are oxidized by HOCl to aldehydes (Fig. 1, 2) [21, 22].

(3) Hydrazines and amides are chlorinated under the action of HOCl followed by hydrolysis in an aqueous medium and formation of carbonyl compounds (Fig. 1, 3) [16, 22].

(4) Cu(I) and other metal-containing compounds are oxidized under the action of HOCl (Fig. 1, 4); based on reactions of this type, chemosensors sensitive, for example, to Cu(II) have been developed for indirect detection of HOCl [22].

(5) Unsaturated carbon–carbon bonds (–HC=CH–) undergo the reaction of electrophilic addition of HOCl with the formation of chlorohydrin isomers [6] and further oxidation to more stable non-chlorinated carbonyl compounds (Fig. 1, 5) [22].

(6) Derivatives of *p*-methoxyphenol and *p*-aminophenol are oxidized by HOCl with the release of benzoquinone and benzoquinoneimine, respectively (Fig. 1, 6) [16, 22, 23].

Classification of Probes according to the Fluorescence Response Type

Fluorescent properties of the probes are important for detecting HOCl. As a result of the interaction of the sensor with the analyte, the intensity of its fluorescence can change as follows:

(1) Decrease: this type of probe is mentioned in the literature under the names “turn-off” [10], “on–off” [16], or “negative” [24].

(2) Increase: this type of probes is called “turn-on” [13], “off–on” [16, 25], or “positive” [24].

(3) Or decrease at one and increase at another wavelength of emission or excitation: their most common name is “ratiometric” [16] or, less often, “switch” probes.

Historically, the first type of chemosensors to appear were the turn-off probes. Such molecular probes lose their fluorescent properties upon interaction with HOCl (Fig. 2a, 1). If the chemosensor does not response to excitation or its fluorescence intensity is extremely low, while the product formed upon reaction with HOCl has fluorescence, the intensity of

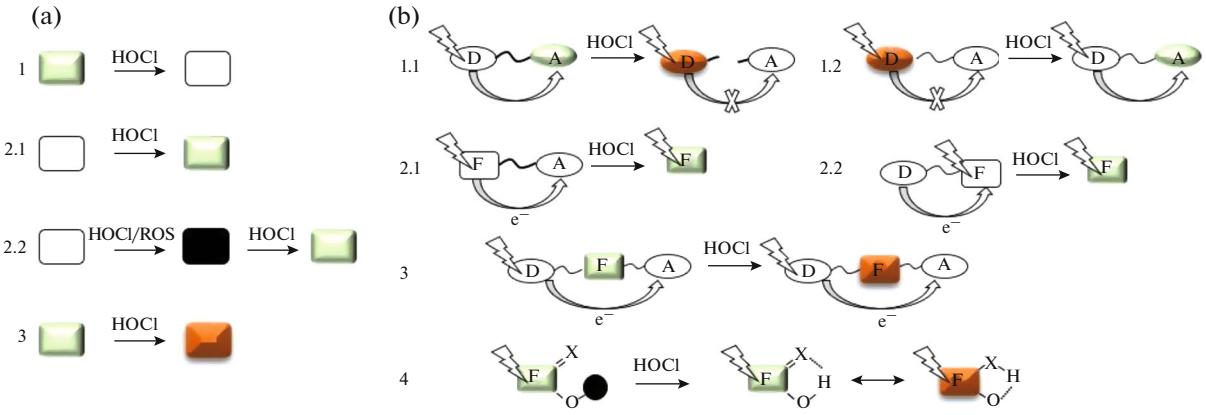

Fig. 2. Types of fluorescent response of the sensors. (a) General view of the types of fluorescent response: (1) turn-off; (2.1) turn-on; (2.2) "double lock"; (3) switching. (b) Modes of changes in the fluorescent response: (1.1) FRET off; (1.2) FRET on; (2.1) a-PET; (2.2) d-PET; (3) ICT; (4) ESIPT. "F" is a fluorophore, "D" is a donor, "A" is an acceptor. With modifications and additions from Gao et al. [27]. See text for explanations.

which is many times higher than the background level, then the sensor is referred to as the turn-on type (Fig. 2a, 2.1). "Turning on" of the probe can occur by direct oxidation to a fluorescent product or by release of a blocked fluorophore. A situation is possible when the probe initially needs to be "activated"; then, upon reaction with the analyte, it passes into the fluorescent form – such a system is called the "double lock" (Fig. 2a, 2.2) [26]. If the interaction with HOCl causes a shift in the spectral range of the excitation or emission spectra, then such probes are of the "switch" type (Fig. 2a, 3). Most often, switch-type probes are characterized by changes in the emission spectra.

Along with the type of the sensor, the mechanism (if established) of changing its fluorescent properties is also indicated: fluorescent resonance energy transfer (FRET), photoinduced electron transfer (PET), intramolecular charge transfer (ICT), or excited state intramolecular proton transfer (ESIPT; Fig. 2b) [27].

FRET is the phenomenon of nonradiative energy transfer from donor D to an acceptor A (Fig. 2b) due to long-range dipole–dipole interactions. The efficiency of FRET strongly depends on the degree of overlap between the absorption (excitation) spectrum of A and emission spectrum of D. The FRET process before the interaction of the chemosensor with HOCl can be either active with subsequent inactivation (FRET off; Fig. 2b, 1.1) or blocked with subsequent activation (FRET on, Fig. 2b, 1.2). Probes designed according to the FRET principle can belong to all three types (turn-on, turn-off, or switch), however, they are most often used as the switch probes, where both the donor and the acceptor act as fluorophores [27, 28]. In recent years, data on a new mode of energy transfer between D and A, similar to FRET, yet devoid of some of its shortcomings, have appeared. For this type of transfer, there is no need for the effective overlap of the emission spectrum of D and absorption spectrum of A; the transfer efficiency does not depend significantly on the distance between D and A, due to which the rate of nonradiative energy transfer increases, and a large pseudo-Stokes shift is observed.

It is assumed that the process of energy transfer occurs through an electronically conjugated rigid linker of the π system (phenyl residues, acetylene, oxidazole component) and is called through bond energy transfer (TBET), although this is not yet fully understood. More details on this how this works and probes based on it can be found, for example, in the review by Cao et al. [29].

PET is a photoinduced electron transfer phenomenon often used in the design of the turn-on type probes. Probes based on PET can be divided into a-PET and d-PET. a-PET is a process of electron transfer from an excited fluorophore F to an electron-deficient acceptor A (Fig. 2b, 2.1), which causes quenching of the fluorescence of F; it is called oxidative PET. d-PET is the transfer of electrons from donor D to the excited fluorophore F (Fig. 2b, 2.2); it causes the reduction of the fluorophore, as well as fluorescence quenching, and is called reductive PET. When the probe reacts with HOCl, the energy levels of the donor and acceptor shift relative to each other (for d-PET, the donor and fluorophore; for a-PET, the acceptor and fluorophore), which leads to blocking of the PET process and an increase in fluorescence intensity [27, 28].

Probes operating according to the ICT principle contain D and A electrons in a single molecule at different ends of fluorophore F (Fig. 2b, 3). The fluorophore itself can also be used as a donor or an acceptor. The excited state of the probe has larger dipole moment compared to the ground state. When the solvate shell rearranges, the energy levels of the ground and excited states converge, and fluorescence with a wavelength much higher than that of the exciting radiation is observed. When the probe reacts with HOCl,

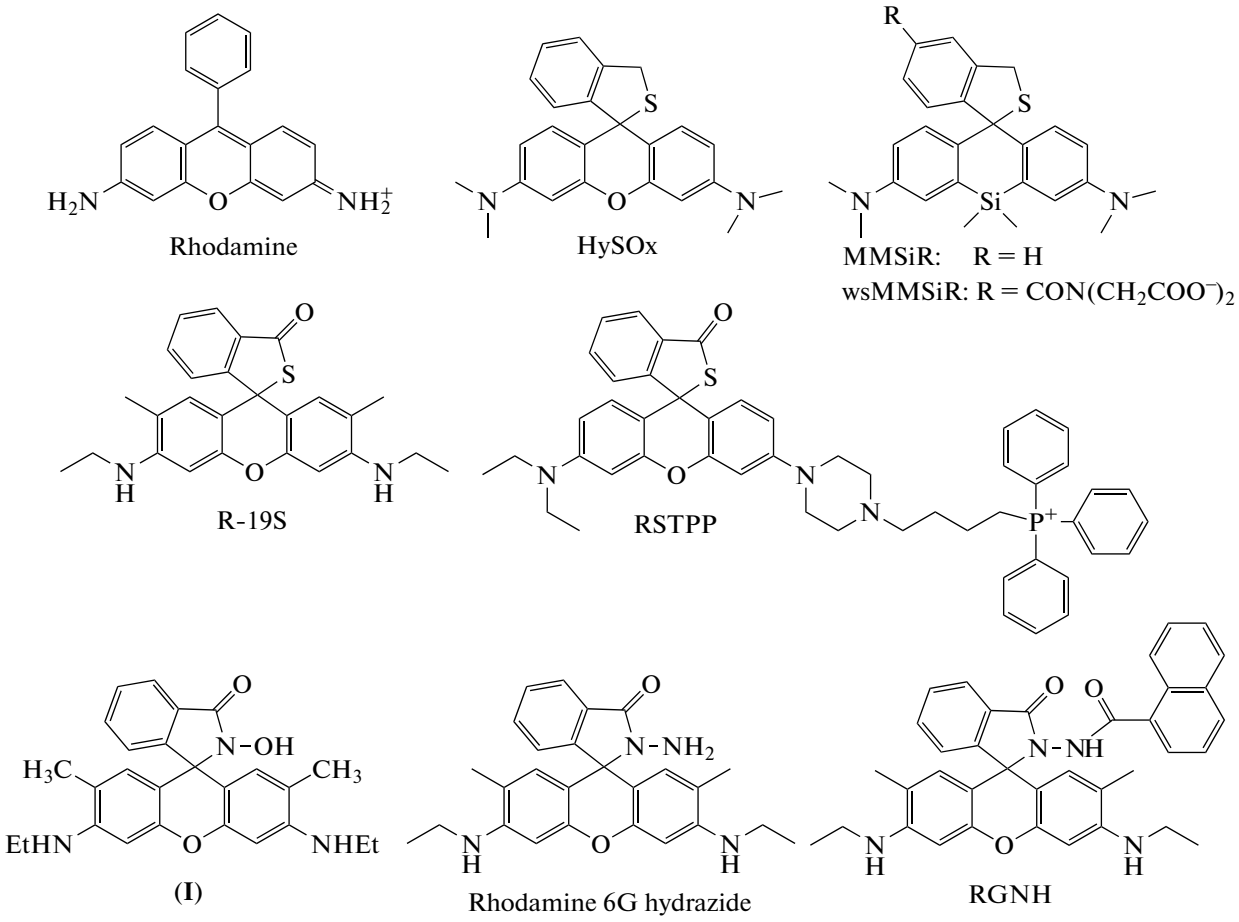

Fig. 3. Structural formulas of rhodamine and rhodamine-based fluorescent probes.

the initial electron density distribution of the sensor is disturbed, which causes a change in the efficiency of the ICT process. A decrease in ICT efficiency leads to a blue shift in fluorescence emission, and conversely, an increase in ICT efficiency leads to a red shift in the fluorescence spectra. On the basis of ICT, probes of the turn-on and switch types are most often designed [27, 28].

ESIPT refers to the phenomenon of transfer of hydrogen atoms from fluorophore F (mainly from hydroxyl or amino groups) to neighboring heteroatoms (mainly to N, O, or S) upon laser excitation (Fig. 2b, 4). ESIPT usually occurs in molecules with a five- or six-membered ring that undergo a tautomerization process accompanied by emission changes due to differences in the structure of the energy levels of the tautomers. The ESIPT strategy can be efficiently applied to the design of the switch type probes [27, 30].

It is often difficult to use the turn-off probes to detect HOCl due to the residual fluorescent signal. The turn-on and switch type probes ensure better spatial resolution and thus are preferable. Switch type sensors are convenient for visualizing reacted and unreacted probes, which helps to minimize errors that can occur due to sample or probe distribution inhomogeneity [31]. However, a small wavelength shift in the emission spectra or the formation of two reaction products with two different excitation wavelengths is often observed, which makes it difficult to use the switch type probes in practice. In addition, they usually have a bulky structure due to the use of several fluorophores, which limits their application [32, 33].

Classification of Probes according to the Fluorophore Type

The selection of suitable low-molecular-weight fluorescent probes for the detection of HOCl in biological assays may be based on the type of their "core," i.e., the fluorophore. There are several main types of fluorophore cores: coumarin, fluorescein, rhodamine and 4,4-difluoro-4-boron-3*a*,4*a*-diaza-*s*-indacene (boron dipyrromethene, BODIPY), 1,8-naphthalimide, cyanine, triazolin, etc. [12, 13, 34]. Thus, the choice of the probe can be made based on the well-studied chemical and photophysical properties of the fluorophore.

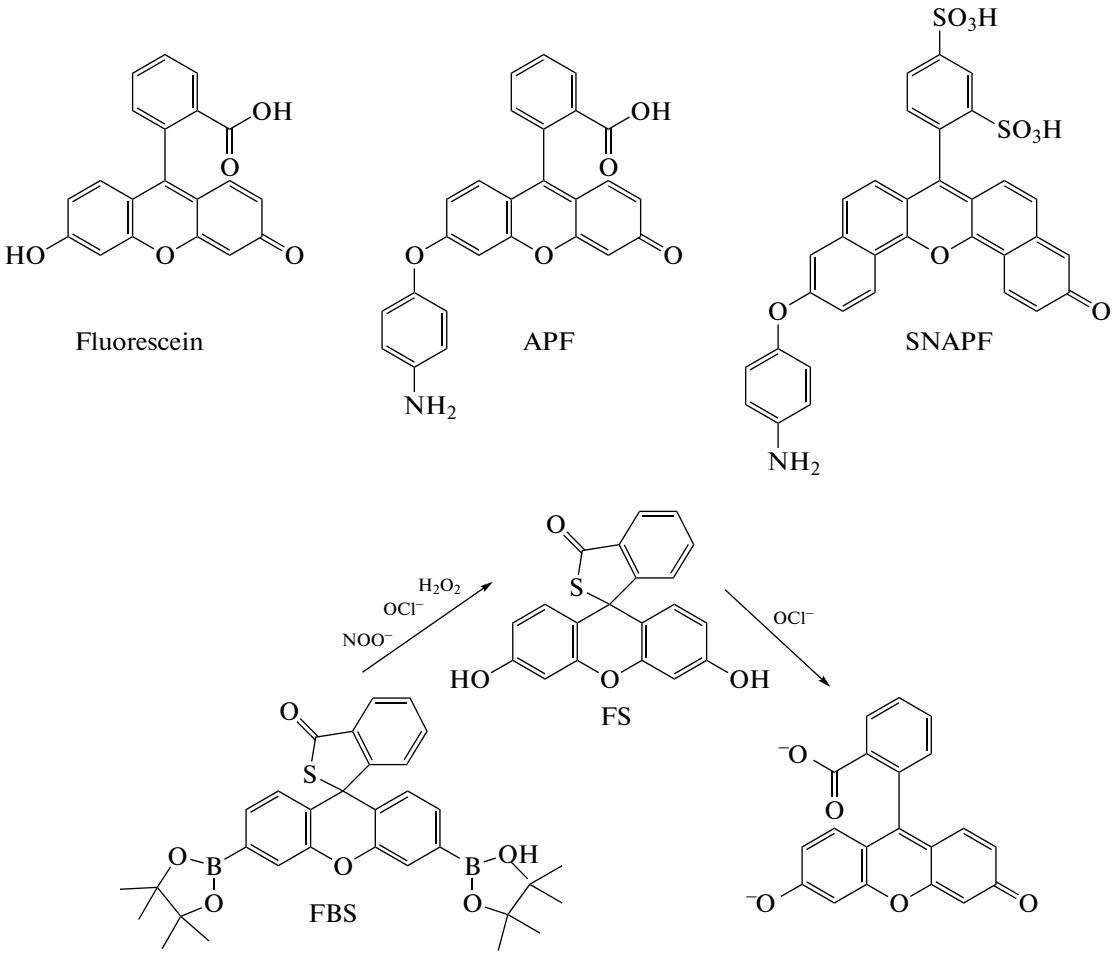

Fig. 4. Structural formulas of fluorescein and fluorescein-based fluorescent probes.

PREREQUISITES FOR THE DEVELOPMENT OF MODERN FLUORESCENT CHEMOSENSORS

The first fluorescent probes to detect ROS production in cells, designed as the turn-off probes, were extremely nonspecific. Later, it seemed reasonable to design more specific chemosensors for detecting HOCl. This process was paralleled by a transition to the synthesis of sensors of the turn-on and switch types. This section presents several developments in this area.

Turn-On and Turn-Off Probes

Rhodamine-based chemosensors. In 2007, a group of scientists led by Kenmoku presented HySOx, a turn-on chemosensor (λ_{ex} = 552 nm; λ_{em} = 575 nm) based on the "S-lock" concept (Fig. 3) [35]. Fluorescence buildup is observed after the sensor is oxidized under the effect of HOCl with the opening of the S-containing ring and transition of the probe to the fluorescent form. HySOx is a sensitive and selective fluorescent probe for HOCl; in addition, the fluorescence intensity of its product is nearly independent of pH in the range of 6.5–9.0. The disadvantages include a low quantum yield and a strong overlap of the absorption and emission spectra [35]. In 2011, based on HySOx, a number of Si-containing analogs (MMSiR and its more hydrophobic derivative wsMMSiR, Fig. 3) were synthesized; their fluorescence intensity in the near infrared region of the spectrum (λ_{ex} = 652 nm; λ_{em} = 770 nm) increases upon reaction with HOCl [36]. HySOx and its modifications were successfully tested in the course of visualization of HOCl production in neutrophil phagosomes activated by opsonized zymosan [35, 36]. They also revealed in vivo HOCl production in a mouse model of peritonitis induced by intraperitoneal injection of zymosan and phorbol 12-myristate 13-acetate (PMA) [36].

In 2011, Chen and coauthors produced another structural analog of HySOx, R-19S (λ_{ex} = 510 nm; λ_{em} = 545 nm) (Fig. 3) [37]. This turn-on probe showed good sensitivity and selectivity of HOCl detection with an optimum pH of ~6. This chemosensor allowed for detection of HOCl production in human and mouse neutrophils by confocal microscopy and

flow cytometry, as well as in the intestinal epithelium of *Drosophila melanogaster*, induced by oral administration of a microbial extract to the insects [37]. In 2015, the RSTPP probe was introduced; it is another structural analog of HySOx of the turn-on type (λ_{ex} = 553 nm; λ_{exp} = 580 nm) (Fig. 3) [38]. The main feature of this probe is the triphenylphosphonium cation, which ensures RSTPP penetration into mitochondria of the cell. The probe demonstrated high sensitivity and selectivity; however, the fluorescence intensity of the product is stable in a narrow pH range of 6–7. To test the sensor, macrophages of the RAW264.7 line (macrophages of mice infected with the Abelson leukemia virus) were used; normally they express MPO at a low level [39] and increase the expression of the enzyme under the effect of a number of stimuli, for example, interferon gamma (IFN-γ) [40]. Production of endogenous HOCl in mitochondria of RAW264.7 macrophages induced by sequential incubation of cells with lipopolysaccharides (LPS) and PMA was demonstrated by confocal microscopy using the chemosensor. Also, production of HOCl by RAW264.7 cells during their incubation with *Escherichia coli* was shown [38].

In 2009, a group of scientists led by Yang proposed a turn-on probe based on rhodamine 6G, compound (**I**) (Fig. 3) [41]. In the initial state, compound (**I**) is in a nonfluorescent spirocyclic form. The hydroxamic acid residue is the HOCl reaction site; chlorination and elimination of HCl yields the open form of rhodamine 19 (R19). This chemosensor is characterized by a short reaction time (the fluorescence intensity reaches a plateau in 20 s), high sensitivity (an increase in the fluorescence intensity is observed when as little as 25 nM HOCl is added), and high selectivity with respect to HOCl in comparison with other major ROS and RNS. However, the operating pH range turned out to be somewhat shifted to the alkaline region (pH 7.5–10.0, maximum at pH 9.0). The probe was used to visualize exogenous HOCl during its incubation with A549 lung cancer cells and embryos of an aquarium fish *Danio rerio* (the Cyprinidae family) [41].

In 2011, Zhang and coauthors synthesized rhodamine 6G hydrazide, a turn-on type chemosensor (Fig. 3) [42]. In contrast to compound (**I**), here the hydrazide fragment acts as a specific reaction site. *N*-Chlorination of the site under the effect of HOCl followed by elimination of HCl leads to the release of R19 (λ_{exc} = 500 nm; λ_{em} = 550 nm). The advantages of this probe include high sensitivity (LOD 60 nM) and a wide range of linear response (2–400 μM HOCl at pH 7.4). The main disadvantages of the sensor are a significant increase in the fluorescence intensity in the presence of copper ions (Cu^{2+}) and a strong shift of the optimum pH of the probe reaction towards low pH values of 2–5, at which the autofluorescence of the chemosensor significantly increases. Rhodamine 6G hydrazide was used to detect the formation of HOCl in macrophages of the RAW264.7 cell line by confocal microscopy during their incubation with LPS and IFN-γ and subsequent PMA activation (the LPS/IFN-γ/PMA system) [42].

In 2015, the same group of scientists proposed rhodamine 6G naphthoyl hydrazide (RGNH), constructed on the basis of rhodamine 6G hydrazide with a naphthoyl fragment in the amino position of the latter (Fig. 3) [43]. RGNH is also referred to the turn-on probe type. The interaction of RGNH with HOCl leads to the formation of fluorescent R19 in a way similar to that of rhodamine 6G hydrazide (λ_{ex} = 500 nm; λ_{em} = 550 nm). The introduction of the naphthoyl fragment allowed the increase in the selectivity and sensitivity (LOD 9 nM), as compared to rhodamine 6G hydrazide, but the working pH range of the probe turned out to be strongly shifted to the alkaline region (pH 9–12). RGNH was successfully used to detect HOCl production by RAW264.7 cells stimulated with LPS/IFN-γ/PMA by confocal microscopy and flow cytometry [43].

Of the probes mentioned above, only the HySOx probe, also known as BioTracker 574 Red HOCl Dye (Sigma-Aldrich, United States), is commercially available.

Fluorescein-based chemosensors. Aminophenyl fluorescein (APF) was developed by Setsukinai's group in 2003 [44]. Attachment of the electron-enriched 4-aminophenylaryl ether fragment to the fluorescein molecule (Fig. 4) leads to quenching of its fluorescence due to the PET process. Under the action of $^{\bullet}OH$, HOCl/HOBr, or $ONOO^-$, as well as in the presence of horseradish peroxidase/H_2O_2 or MPO/H_2O_2/Cl^- systems, APF is converted to fluorescein by O-dearylation, which is accompanied by an increase in fluorescence intensity (λ_{ex} = 490 nm; λ_{em} = 515 nm). That is, APF acts as a turn-on probe. LOD for $^{\bullet}OH$, $ONOO^-$ and HOCl is 50 nM [45]. APF is used to detect the production of HOCl and HOBr by neutrophils and eosinophils by confocal microscopy [44] and flow cytometry [46]. Its high quantum yield and high sensitivity allow detecting the production of HOCl/HOBr in a suspension of leukocytes obtained immediately after hemolysis of whole blood erythrocytes [46, 47]. However, to assess the selective role of HOCl, relative to other ROS, RHS, and RNS, in the conversion of APF to fluorescein, it is necessary to use a differential approach using the structural analog of APF, hydroxyphenylfluorescein (HPF), which reacts with the same highly reactive compounds as APF, except for HOCl [44].

In 2007, Shepherd and coauthors proposed a modification of the APF to sulfonaphthoaminophenyl fluorescein (SNAPF), which is also a turn-on type sensor. A distinctive feature of SNAPF is the shift of the excitation and fluorescence spectra to the near infrared region (λ_{ex} = 614 nm; λ_{em} = 676 nm) [48]. This probe showed high selectivity and was used to detect

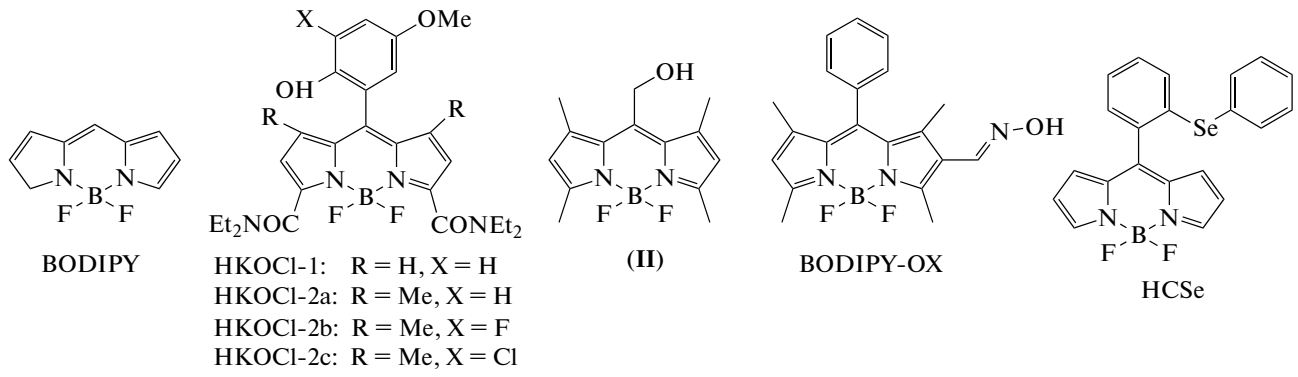

Fig. 5. Structural formulas of BODIPY and BODIPY-based fluorescent probes.

HOCl production by PMA-stimulated human neutrophils and macrophages of mice, transgenic for the gene encoding human MPO, by fluorescence microscopy. In addition, using SNAPF, the presence of HOCl was detected in samples of human arteries with atherosclerotic plaques, as well as in vivo in mice with thioglycolate-induced peritonitis [48].

The double lock concept was implemented by Xu et al. in 2013 in the design of the FBS turn-on probe [49]. The reaction of FBS with H_2O_2, $ONOO^-$, or HOCl yields a weakly fluorescent product, FS, which, in turn, selectively reacts with HOCl to release fluorescein (λ_{ex} = 498 nm; λ_{em} = 523 nm) (Fig. 4). The probe is sensitive and selective for HOCl in the pH range of 7–9. FBS is not oxidized to a fluorophore under the action of $^{\bullet}O_2^-$, $^{\bullet}NO$, $^{\bullet}OH$, hydroperoxides, or peroxyl radicals. FBS was used to visualize the production of HOCl in the gut of drosophila upon oral administration of a bacterial extract to insects [49].

Of the probes based on fluorescein mentioned, only APF and its structural analog HPF (Sigma-Aldrich, United States) are commercially available.

BODIPY-based chemosensors. In 2008, Sun and coauthors designed a probe of the turn-on type HKOCl-1 (Fig. 5) [50]. An increase in the fluorescence intensity of the sensor occurs due to the oxidation of 4-methoxyphenol to benzoquinone in the presence of HOCl, which in turn leads to the loss of the ability of the 4-methoxyphenol residue to quench the fluorescence of the BODIPY core by the PET mechanism (λ_{ex} = 520 nm; λ_{em} = 541 nm). The probe is characterized by high sensitivity and selectivity and a wide operating range of pH 5–8. HKOCl-1 was used to detect the formation of HOCl in the $MPO/H_2O_2/Cl^-$ system, as well as in RAW264.7 macrophages upon their stimulation with LPS/IFN-γ/PMA [50, 51]. However, the probe was subsequently not used in practice due to the reoxidation of the fluorescent product with the formation of a nonfluorescent compound [52].

In 2014, Hu and coauthors developed a number of analogs of HKOCl-1 (HKOCl-2a–c) with additional protection of 4-methoxyphenol with two methyl groups (Fig. 5) [52]. Among them, HKOCl-2b (λ_{ex} = 523 nm; λ_{em} = 545 nm) showed the highest selectivity and sensitivity (LOD 18 nM) with respect to HOCl. Probes HKOCl-2a and HKOCl-2b are characterized by a long time for reaching the fluorescence intensity plateau during their reaction with HOCl (up to 15 min), while for HKOCl-2c this indicator is much lower (3 min). Nevertheless, the fluorescent response for HKOCl-2c is 3 times lower than that for HKOCl-2a and HKOCl-2b. Based on the set of parameters, HKOCl-2b was chosen as the most promising one. It was used to detect HOCl production in RAW264.7 cells stimulated with PMA or zymosan by confocal microscopy. Also, using this probe, HOCl production was shown for the first time in differentiated THP-1 cells (human monocytes derived from an acute monocytic leukemia patient, expressing MPO at a low level [53]), when they were stimulated with PMA or zymosan [52].

A turn off-type probe based on BODIPY with a hydroxymethyl group in the *meso*-position was presented by Gai et al. in 2013 (compound (**II**), Fig. 5) [54]. The fluorescence of the probe is turned off due to the conversion of the hydroxymethyl group into formyl as a result of the oxidation reaction in the presence of HOCl (λ_{ex} = 480 nm; λ_{em} = 525 nm). The sensor demonstrated good selectivity for HOCl compared to $^{\bullet}OH$, $^{\bullet}O_2^-$, H_2O_2, or $NO^{\bullet}$. This probe was tested on the MCF-7 cell line with exogenous introduction of HOCl into the culture medium [54].

In 2013, Emrullahoglu and coauthors proposed a turn-on type probe based on the BODIPY core with an inserted aldoxime group (BODIPY-OX) (Fig. 5) [55]. Under the action of HOCl, fluorescent nitrile oxide BODIPY-CNO is formed (λ_{ex} = 470 nm; λ_{em} = 529 nm). The probe showed high sensitivity (LOD 500 nM) and selectivity, but the fluorescence intensity of BODIPY-CNO strongly depended on pH (optimum at pH 8). Subsequently, it was shown that

BODIPY-CNO is unstable and decomposes into components that could not be identified, which made it impossible to use the probe to detect the formation of HOCl in cell media [55].

Also in 2013, Liu and Wu presented a selenium-containing probe of the turn-on type HCSe (Fig. 5). Initially, HCSe fluorescence is blocked by the PET process. After the oxidation of HCSe under the effect of HOCl, selenium oxide (HCSeO) is formed, in which PET is blocked, which leads to an increase in the fluorescence intensity (λ_{ex} = 510 nm; λ_{em} = 526 nm). The probe is characterized by high sensitivity and selectivity and fast response. The optimum sensor performance lies in the pH range of 6–8. HCSe was used to detect the formation of HOCl in RAW264.7 cells stimulated with PMA [56].

Of the above probes, only the HKOCl-1 probe (Molbase (Shanghai) Biotechnology Co. Ltd, China) is currently produced and available for purchase.

Transition to the Switch Probe Concept

In 2009, Lin et al. for the first time proposed a switch type probe for detecting HOCl. The functioning of this sensor is based on the HOCl-mediated conversion of oxime to aldehyde. However, the optimum reaction of the probe is in the alkaline region (pH > 9), which makes the probe unsuitable for detecting HOCl production in cell systems [21]. In 2012, the same group of scientists proposed a strategy for the cyclization of rhodamine thiosemicarbazides to rhodamine oxadiazoles under the effect of HOCl as the basis for the switch probes [31]. Thus, a rhodamine-coumarin sensor was created (compound (**III**), Fig. 6), in which the switching of the fluorescence intensity from coumarin (λ_{ex} = 414 nm; λ_{em} = 473 nm) to rhodamine (λ_{ex} = 414 nm; λ_{em} = 594 nm) channels occurs due to FRET (λ_{ex} = 414 nm; λ_{em} = 594/473 nm). The probe showed high selectivity and sensitivity to HOCl (LOD 52 nM), fast fluorescence intensity growth till a plateau (within 3 min). In this case, the change in the fluorescence of the probe strongly depends on pH (optimum reaction at pH 6). This rhodamine–coumarin sensor was successfully used to detect HOCl production by RAW264.7 cells upon their stimulation with LPS/PMA [31].

In 2013, Long's group proposed the HRS1 probe [57]. It contains coumarin- and rhodamine-based fluorophores linked together by diacylhydrazine, which acts as the HOCl reaction site. HRS1 is characterized by fluorescence in the spectral region of coumarin (λ_{ex} = 410 nm; λ_{em} = 501 nm). After the reaction of HRS1 with HOCl, both coumarin and rhodamine fragments are released. Thus, the sensor can be considered as a switch probe for coumarin (λ_{ex} = 410 nm; λ_{em} = 464/501 nm) and a turn-on probe for rhodamine (λ_{ex} = 554 nm; λ_{em} = 578 nm). The probe showed high selectivity and sensitivity to HOCl (LOD 24 nM) in a cell-free medium and rapid fluorescence intensity growth to plateau (within 1 min). However, HRS1 has not received further application because the presence of both fluorophores with different fluorescence excitation channels needs to be taken into account [57].

In 2014, Zhang and coauthors proposed another switch type rhodamine–coumarin probe (compound (**IV**); Fig. 6). Like HRS1, diacylhydrazine acts as the HOCl reaction site. The switching process occurs according to the FRET mechanism (λ_{ex} = 410 nm; λ_{em} = 580/470 nm). The sensor is characterized by selectivity for HOCl and a fast response, yet a high LOD for HOCl (170 μM) and strong dependence of the fluorescence intensity on pH (optimum at pH 9.3) should be noted as disadvantages. In addition, the reaction product of the probe with HOCl (coumarin–rhodamic acid) undergoes chlorination followed by cyclization under the action of HOCl, which leads to blockade of FRET and an increase in fluorescence in the coumarin detection channel. A chemosensor was used to detect HOCl production by RAW264.7 cells upon their stimulation with LPS [58].

In 2014, a group led by Wang synthesized a switch probe based on coumarin (compound (**V**); Fig. 6) [59]. For the first time, *N*-alkylpyridinium, which is oxidized to *N*-alkylpyridone under the effect of HOCl, was used as the recognition site in this sensor. In this case, the ICT process is blocked, which is accompanied by a shift in the wavelengths in the emission spectrum (λ_{ex} = 420 nm; λ_{em} = 488/631 nm) to the blue region. The probe is characterized by high selectivity, relatively high sensitivity to HOCl (LOD 93 nM), and a short reaction time; however, the fluorescence intensity strongly depends on pH (optimum at pH 7.5–11.0). The probe was used to determine the concentration of HOCl in river water samples, as well as to register the production of HOCl in RAW264.7 cells upon their activation with PMA.

In 2015, Goswami and coauthors proposed a TAM probe based on triphenylamine as a switch-type sensor for the detection of HOCl (Fig. 6) [60]. Diaminomaleonitrile (DAMN; Fig. 6) is linked to the probe backbone via an imino group, which serves as the HOCl reaction site. After TAM oxidation under the effect of HOCl, the DAMN fragment is cleaved off, which is accompanied by a shift in the fluorescence emission spectrum of the probe (λ_{ex} = 430 nm; λ_{em} = 485/630 nm) to the blue region. The probe is characterized by high sensitivity (LOD 70 nM), selectivity, a short reaction time with HOCl (reaching a plateau in 100 s), high quantum yield (0.86), and a wide operating pH range (2.0–10.5). However, this sensor is characterized by strong solvatochromism (a shift in the fluorescence emission spectra depending on the polarity of the solvent). TAM was used to detect exogenous HOCl in human peripheral blood mononuclear cells by confocal microscopy [60].

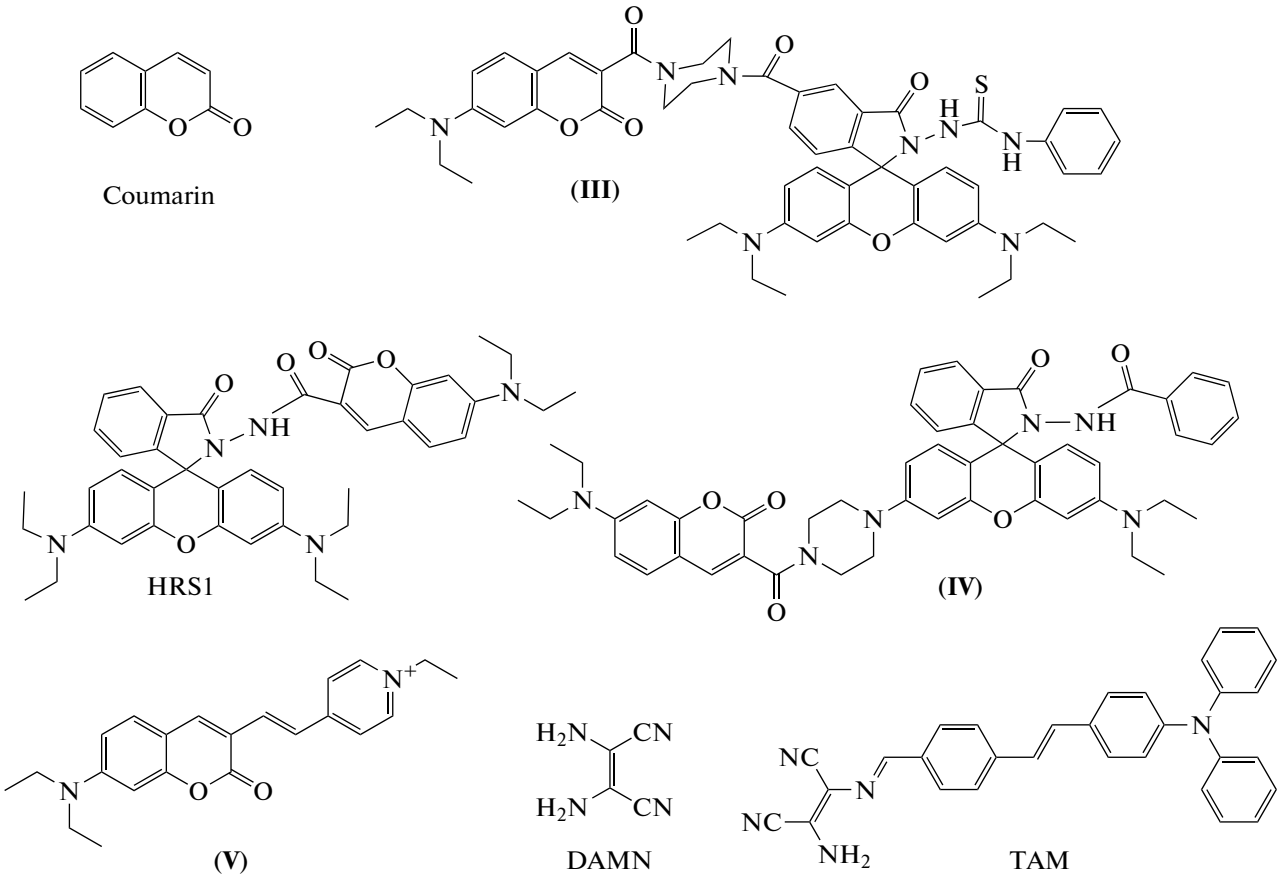

Fig. 6. Structural formulas of ratiometric fluorescent probes.

None of the switch type probes mentioned are commercially available.

RECENT ADVANCES IN THE DEVELOPMENT OF SMALL-MOLECULE FLUORESCENT PROBES TO REGISTER HOCl

In recent years, active work has been performed on the design of small-molecule probes for detecting HOCl based on known fluorophores with various modifications to achieve desired properties. Of particular interest are probes characterized by not only high selectivity and sensitivity, but also fast response for the possibility to study the kinetics of HOCl formation. Also, the efforts of scientists are focused on the possibility of two-photon excitation of probes and/or registration of their fluorescence in the near infrared range. Switch-type sensors have received a boost.

Coumarin-Based Probes

At the beginning of 2018, a group of scientists led by Liu proposed a turn-off type probe CMOS based on coumarin (Fig. 7) [61]. 1,3-Oxothiolane serves as the HOCl reaction site. Turn off of fluorescent response (λ_{ex} = 405 nm; λ_{em} = 480 nm) occurs due to the formation of a nonfluorescent CMOS oxidation product CMCHO under the action of HOCl. It was also shown that in the presence of cysteine or homocysteine (Cys/Hcy), CMCHO undergoes thioacetalization with the formation of CMCys or CMHcy (Fig. 7), which is accompanied by a slow increase in the fluorescence intensity at a wavelength characteristic of CMOS. Thus, this probe is an example of a transition of the on–off–on type. CMOS is characterized by a fast response (5 s), high sensitivity (LOD 21 nM), and selectivity; the optimum reaction of the probe is observed in the pH range 4.0–6.5. The probe was used to visualize exogenous HOCl in ovarian cancer (SKVO-3) cells. Confocal microscopy showed a decrease in the CMOS fluorescence intensity in SKVO-3 cells upon the introduction of HOCl, as well as restoration of the fluorescence intensity in the presence of Cys/Hcy. Based on the data obtained, the authors concluded that CMOS can be used to study the processes of thiol oxidation and reduction in biological systems [61].

In 2019, Jin and coauthors proposed two probes of the switch and turn-on types with a coumarin core, BCO and BETC, respectively (Fig. 7) [62]. Switching BCO (λ_{ex} = 372 nm; λ_{em} = 430/460 nm) and turning

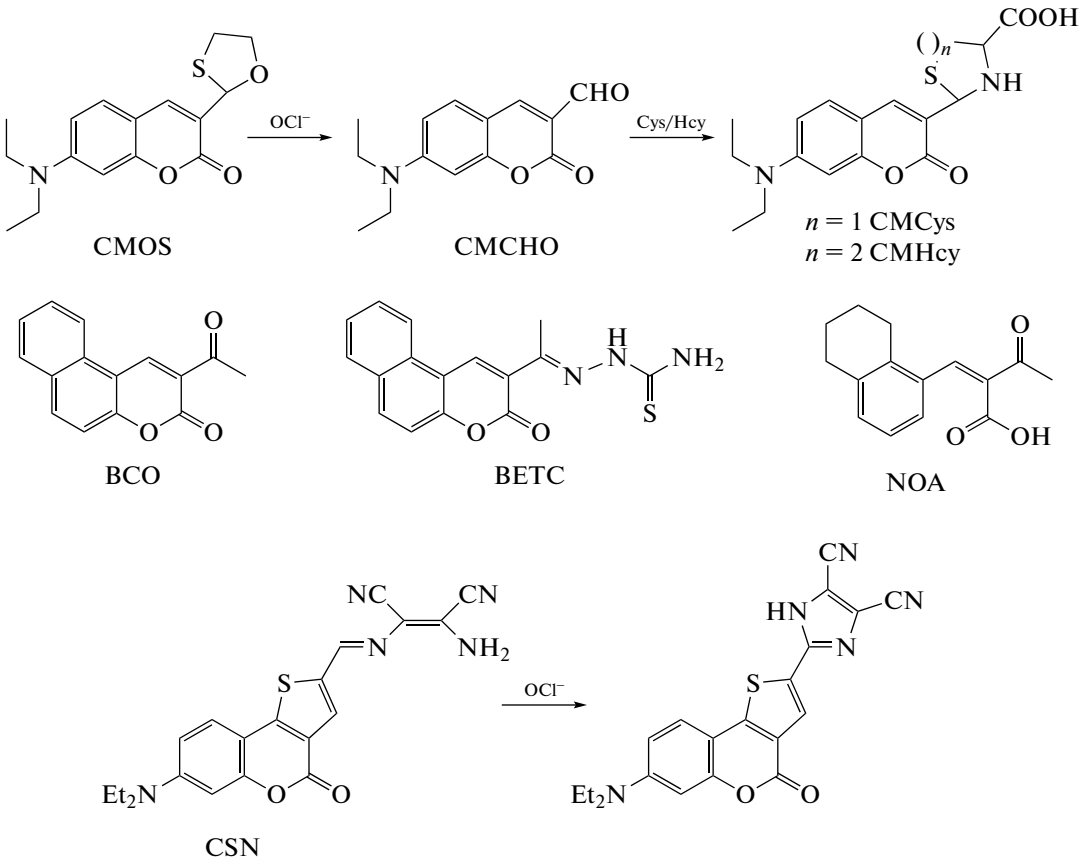

Fig. 7. Structural formulas of new fluorescent probes based on coumarin.

on BETC (λ_{ex} = 350 nm; λ_{em} = 440 nm) fluorescence is based on the oxidation of C=O (in the case of BCO) or C=O and C=N bonds (in the case of BETC) under the effect of HOCl with the formation of a common end product (NOA, Fig. 7). Both probes showed high sensitivity (LOD 154 nM for BCO and 32 nM for BETC) and selectivity for HOCl. However, BCO has a small shift in fluorescence emission wavelengths, which makes it difficult to use. The chemosensors were used to visualize exogenous HOCl in human hepatocellular carcinoma (HepG2) cells using confocal microscopy [62].

In early 2020, Shi's group presented a coumarin-based switch probe CSN, in which DAMN was chosen as the HOCl reaction site [63]. Switching of the probe (λ_{ex} = 413 nm; λ_{em} = 470/640 nm) occurs due to the oxidation and cyclization of DAMN in the presence of HOCl. The probe is characterized by a large blue shift, high sensitivity (LOD 94 nM), and selectivity to HOCl; the optimum fluorescence intensity of the probe was observed in the pH range of 6.6–8.6. The disadvantage of CSN is its weak photostability (a significant change in the fluorescent characteristics of CSN was observed 30 min after the start of probe irradiation with a xenon lamp). Despite this, a gradual increase in the fluorescence intensity of the probe in the blue registration channel relative to the red channel in HeLa cells (cervical cancer cells) after incubation with HOCl was shown. The chemosensor was also successfully used to detect HOCl production by RAW264.7 cells by confocal microscopy during stimulation with LPS [63]. None of the coumarin-based probes listed in this subsection are commercially available.

Fluorescein-Based Probes

In 2016, Hu and coauthors proposed a modification of the HPF probe with the introduction of two chlorine atoms in the *ortho* position (2,6-dichlorophenol fragment), HKOCl-3 (Fig. 8) [64]. PET provides a low background level of HKOCl-3 fluorescence. The sensor fluorescence turns on due to the reaction of oxidative O-dearylation of 2,6-dichlorophenol (λ_{exc} = 490 nm; λ_{em} = 527 nm). HKOCl-3 has extremely high sensitivity (LOD 0.33 nM), selectivity, and fast response to HOCl; its disadvantage is the strong dependence of the fluorescence intensity of the product on the pH of the medium (optimum is achieved in a narrow pH range of 7.0–7.5). The chemosensor was used to register HOCl production by confocal microscopy in RAW264.7 and THP-1 cell

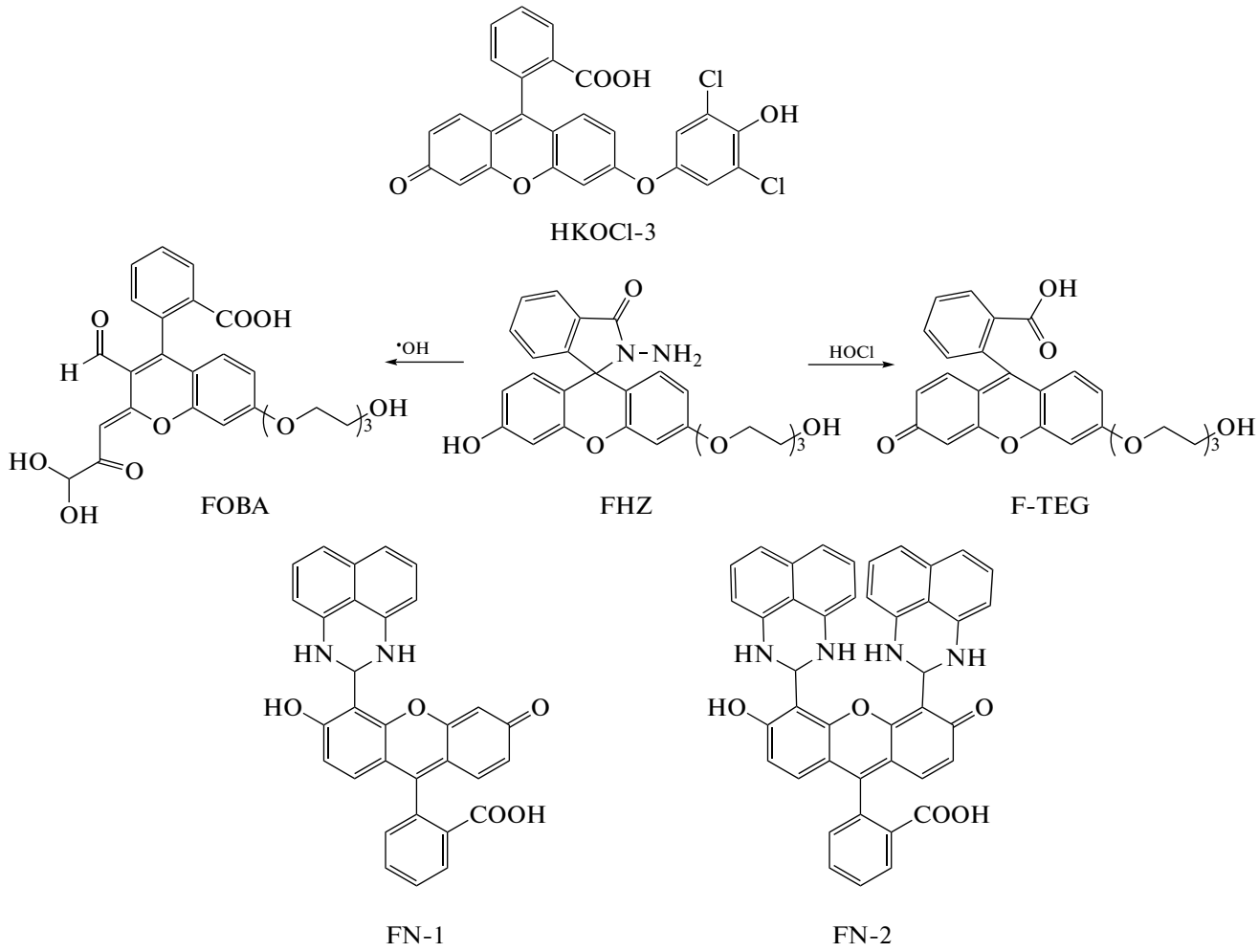

Fig. 8. Structural formulas of new fluorescent probes based on fluorescein.

lines, human neutrophils, and in mouse microglial cells (BV-2 expressing MPO upon exposure to a number of stimuli [65, 66]) upon PMA stimulation. In addition, HKOCl-3 is suitable for registering endogenous HOCl production by flow cytometry and fluorimetry. This probe is also effective in fluorescence microscopy for detecting the production of endogenous HOCl in vivo in live intact embryos of aquarium fish *Danio rerio* at different stages of their development [64].

In 2016, Zhang's group presented an FHZ turn-on chemosensor based on fluorescein (Fig. 8) [67]. The probe has two reaction sites: one for ·OH and another one for HOCl. In the presence of only ·OH, hydroxylation of one of the six-membered aromatic rings occurs, followed by its cleavage, as well as cleavage of the five-membered FHZ ring to form the final product FOBA (Fig. 8). In the presence of only HOCl, the reaction proceeds without breaking the six-membered aromatic ring with the formation of the F-TEG product (Fig. 8). Due to the spectral differences between the resulting products, it is possible to simultaneously register an increase in the fluorescence intensity under the action of ·OH and HOCl in different channels: blue (λ_{ex} = 410 nm; λ_{em} = 486 nm) for ·OH and green (λ_{ex} = 490 nm; λ_{em} = 520 nm) for HOCl. FHZ reacts with simultaneously present ·OH and HOCl for 2–3 min, increasing the fluorescence intensity by a factor of 19 in the blue channel and by a factor of 35 in the green channel. In the case of HOCl, it has been shown that fluorescence is turned on due to the blocking of the PET process [67, 68]. FHZ is selective for ·OH and HOCl and has been tested in HeLa cells with exogenous addition of oxidants and on RAW264.7 cells with PMA activation. FHZ is distributed both in the cytoplasm and mitochondria of the cells. High biocompatibility of the probe has been demonstrated. Selective accumulation of spontaneously formed ·OH and HOCl in organs (intestine, liver, pronephros) of live embryos of aquarium fish *Danio rerio* was shown [67].

In 2019, Lv's group presented two turn-on probes based on fluorescein, FN-1 and FN-2 (Fig. 8) [69]. Both probes were obtained by condensation of amino groups of 1,8-diaminonaphthalene with aldehyde

groups of mono- (in the case of FN-1) or bis- (in the case of FN-2) fluorescein aldehyde. The nitrogen of the imino group thus obtained (–NH–) acts as a target for HOCl. When the probes react with HOCl, fluorescein mono- and bisaldehyde are formed (in the case of FN-1 and FN-2, respectively). The reaction is accompanied by the buildup of fluorescein fluorescence (λ_{ex} = 490 nm; λ_{em} = 529 nm) due to PET blocking. The fluorescence quantum yield of products of the reaction between the probes and HOCl is 3–4 times lower than that of fluorescein. FN-1, compared to FN-2, has a higher background fluorescence level and a slower rate of reaction with HOCl. The optimum reacting range is achieved at pH 7–10 for FN-1 and pH 6–10 for FN-2. Both sensors are more specific but less sensitive to HOCl than APF (LOD 210 and 230 nM for FN-1 and FN-2, respectively). FN-1 and FN-2 were used to register HOCl production upon addition of exogenous H_2O_2 to HeLa cells preincubated with NaCl and MPO [69].

Of the fluorescein-based probes listed in this subsection, HKOCl-3 (MedChemExpress, United States) and FHZ (Sigma-Aldrich, United States) probes are available for purchase.

Phenoxazine-Based Probes

In 2016, a phenoxazine-based dye, celestine blue B (CB), was proposed as a turn-on type probe for detecting HOCl production (Fig. 9) [70]. Fluorescence of CB in the visible region of spectrum is barely observed at all; the reaction with HOCl leads to the formation of CB glycol (Fig. 9) [71]. The reaction of CB with HOCl is accompanied by an increase in the fluorescence intensity in the orange region of the spectrum (λ_{ex} = 460 nm; λ_{em} = 590 nm). The probe is characterized by selectivity for HOCl, HOBr, as well as halogenated taurine derivatives and proteins. The chemosensor has a high sensitivity to HOCl (LOD 32 nM), photostability, high reaction rate (fluorescence intensity plateau is reached within 30 s), and a large Stokes shift. A significant increase in the fluorescence intensity (by a factor of ~100) is observed in the pH range of 7.0–7.5, while the background fluorescence level is low and barely changes in the pH range of 2.2–8.0. CB showed an increase in fluorescence intensity in flow cytometry and confocal microscopy assay of human neutrophils upon PMA stimulation [70]. Moreover, CB can be used for the kinetic analysis of HOCl production in suspensions of neutrophils activated with PMA, a chemotactic peptide *N*-formylmethionyl-leucylphenylalanine, and plant lectins with various carbohydrate specificities (in the presence of cytochalasin B). The chemosensor was successfully tested in the study of the effect of drugs on the production of HOCl by human neutrophils [70–72].

In 2019, Choi and coauthors presented the RT-1 turn-on probe based on a carbonodithioate derivative of resorufin (Fig. 9) [73]. Hydrolysis of the carbonodithioate fragment under the action of HOCl leads to the release of fluorescent resorufin (λ_{ex} = 550 nm; λ_{em} = 587 nm). The probe showed high sensitivity (LOD 2.18 nM), selectivity to HOCl, but a relatively low reaction rate with HOCl (fluorescence intensity reached a plateau within 3 min). The disadvantages of the probe include a drop in the fluorescence intensity of resorufin in the presence of bromide and iodide ions, as well as a strong dependence of the ratio of the fluorescence intensity of resorufin to the fluorescence intensity of RT-1 on the pH value of the medium (optimum at pH 8). RT-1 was used to visualize exogenous HOCl in RAW264.7 and HeLa cell lines [73].

In 2020, Yang et al. presented two probes of the turn-on type—BR-O [74] and BR-1 [75]—having *N*,*N*-dimethylcarbonyl and *N*,*N*-dimethylthiocarbonyl residues as HOCl reaction sites, respectively (Fig. 9). Both chemosensors are oxidized by HOCl with the release of an unstable reduced form of *bis*-dimethylaminophenoxazine, which is rapidly hydrolyzed and oxidized to the final fluorophore, oxazine 1 (λ_{ex} = 610 nm; λ_{em} = 670 nm). Both probes showed selectivity for HOCl compared to ROS and RNS, a fairly fast response (fluorescence intensity plateau is reached within 7 and 2.5 min for BR-O and BR-1, respectively), stability of the fluorescent signal in the pH range of 5–8, and high sensitivity (LOD 19 and 11 nM for BR-O and BR-1, respectively). The disadvantage of these sensors is the strong overlap of the absorption and emission spectra (the Stokes shift was 20 nm for both probes). BR-O and BR-1 showed an increase in fluorescence intensity when exogenous HOCl was added to the RAW264.7 cell culture. In addition, using these probes, spontaneous formation of HOCl in human acute promyelocytic leukemia cells (HL-60 line expressing MPO at a high level [53]) and suppression of this process in the presence of an MPO inhibitor, 4-aminobenzoic acid hydrazide, were revealed [74, 75]. BR-1 was used to detect HOCl formation in a mouse model of arthritis of the knee joint [75] induced by injection of λ-carrageenan mucopolysaccharide, a known arthritis inducer in rats [76].

Also in 2020, a group of scientists led by Zheng presented two modifications of the BR-O probe: BC-2 and BC-3 (Fig. 9) [77]. The target for HOCl in these sensors is the carbon atom of the amide group. As in the case of BR-O and BR-1, the interaction of BC-2 and BC-3 with HOCl leads to the cleavage of the amide bond, releasing the reduced bis-dimethylaminophenoxazine, which then rapidly transforms into the oxidized form; this in turn is accompanied by an increase in the fluorescence intensity of oxazine 1 (λ_{ex} = 620 nm; λ_{em} = 669 nm). BC-2 and BC-3 are sensitive (LOD 20 and 11 nM, respectively) and selective for HOCl compared to ROS and RNS. At the same time, the increase in fluorescence intensity is three times greater in the case of the interaction of HOCl with BC-3 in comparison with BC-2. A signif-

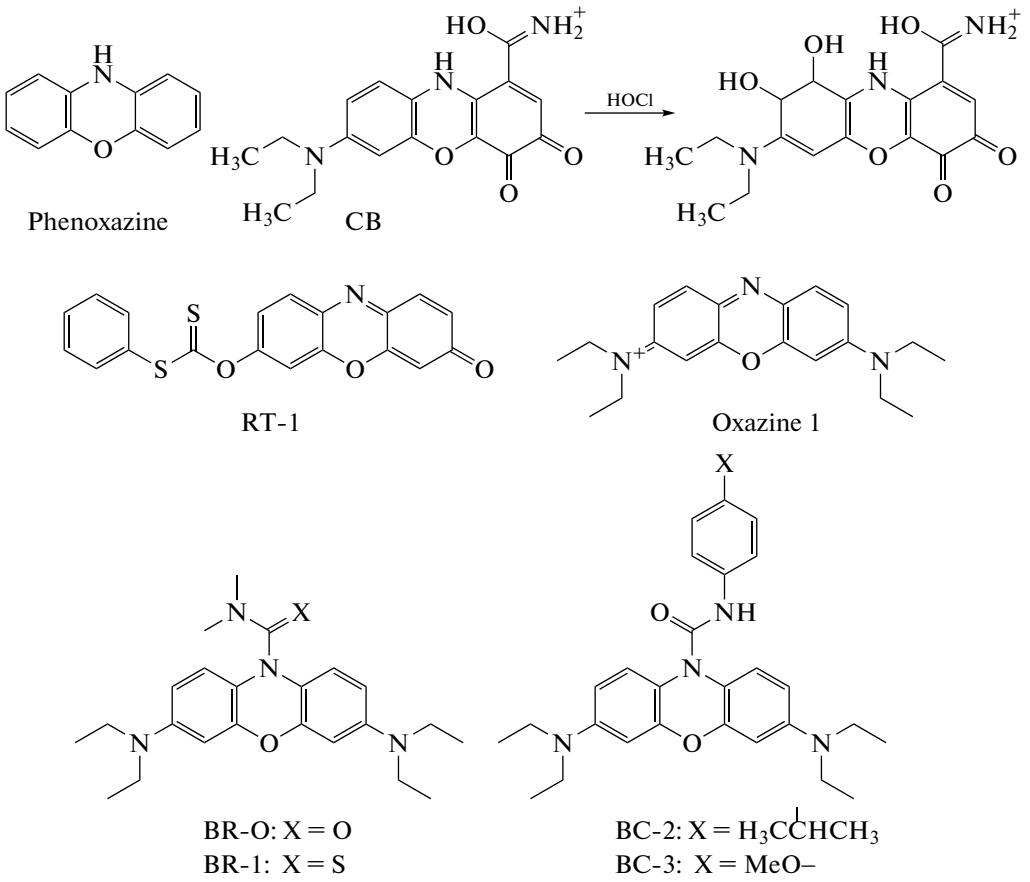

Fig. 9. Structural formulas of phenoxazine and new phenoxazine-based fluorescent probes.

icant improvement of these modifications compared to the BR-O and BR-1 probes is a decrease in the time to reach the fluorescence intensity plateau after the addition of HOCl (30–50 s). BC-3 was used to detect spontaneous HOCl production in HL-60 cells, as well as in a model of arthritis in mice after injection of λ-carrageenan [77].

Of these phenoxazine-based probes, only the CB probe (Sigma-Aldrich, United States; Thermo Fisher Scientific, United States) is commercially available.

Rhodol-Based Probes

Rhodol is a hybrid fluorophore based on fluorescein and rhodamine (Fig. 10); its derivatives (rhodafluors) are also used as fluorescent probes for detecting HOCl. In 2018, Zhang et al. presented the RO610 turn-on probe based on rhodol [78]. DAMN was chosen as the reaction site. Under the action of HOCl, the DAMN residue is cleaved off, which is accompanied by the buildup of rhodol fluorescence (λ_{ex} = 535 nm; λ_{em} = 577 nm). RO610 has a high sensitivity (LOD 29 nM), selectivity for HOCl in comparison with ROS and RNS, and a rapidly reached plateau of the kinetic curve of fluorescence intensity (within 30 s). However, the chemosensor has a narrow pH range for detection (7.0–8.5). RO610 has been tested for visualization of exogenous HOCl on the A549 cell line, as well as intraperitoneal injection of HOCl in mice. In addition, the possibility to register the formation of endogenous HOCl in vivo in a model of peritonitis in mice was shown both upon introduction of zymosan and without additional stimulation [78].

In 2020, Bai and coauthors constructed the turn-on type probes HKOCl-4 and its derivatives, HKOCl-4r and HKOCl-4m, based on rhodol (Fig. 10) [79]. In all three probes, the 2,6-dichlorophenol residue was used as the site for the reaction with HOCl. The transformation of sensors into a fluorescent form occurs due to the *O*-dearylation reaction (λ_{ex} = 530 nm; λ_{em} = 557 nm). HKOCl-4 is extremely sensitive (LOD 9 nM) and selective for HOCl. The increase in fluorescence intensity occurs rapidly (a plateau is reached within 30 s), however, a strong dependence of the fluorescence intensity on pH is observed (maximum at pH 8). HKOCl-4r and HKOCl-4m were developed to improve probe penetration into cells and detect HOCl production in mitochondria. For example, a dimethyl

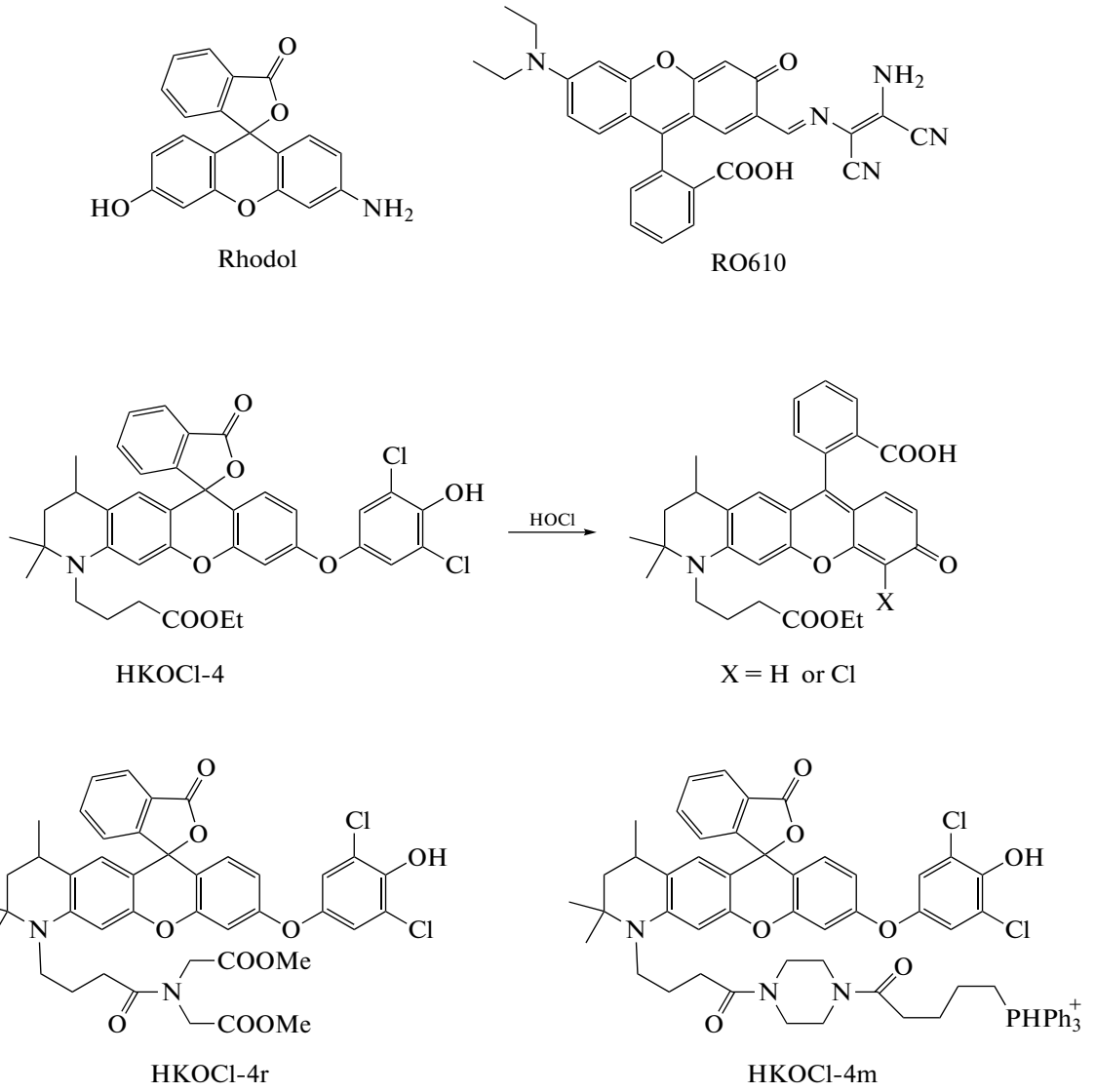

Fig. 10. Structural formulas of rhodol and new rhodol-based fluorescent probes.

ester group, which can be hydrolyzed by cell esterases, was introduced into HKOCl-4r, and a cationic mitochondria-targeted fragment based on triphenylphosphonium was introduced into HKOCl-4m (Fig. 10). Confocal microscopy using HKOCl-4r showed the formation of HOCl in RAW264.7 cells upon stimulation with PMA, as well as by LPS/IFN-γ; in addition, the presence of HOCl in the brain tissues of rats with ischemic damage was shown. Using confocal microscopy and flow cytometry with HKOCl-4m, HOCl was visualized in mitochondria of RAW264.7 cells stimulated with PMA or LPS/IFN-γ [79].

Of these rhodol-based probes, HKOCl-4 and HKOCl-4m are commercially available.

1,8-Naphthalimide-Based Probes

Although 1,8-naphthalimide has been used in the design of HOCl probes in the past, its popularity has increased in recent years. In 2017, a group led by J. Li synthesized a turn-on type probe based on 1,8-naphthalimide, compound (**VI**) (Fig. 11) [80]. HOCl oxidizes the hydroxyl group of this probe to carbonyl, which is accompanied by an increase in the fluorescence intensity (λ_{ex} = 414 nm; λ_{em} = 523 nm). The chemosensor is characterized by a relatively low sensitivity (LOD 2.66 μM), a large range of linear dependence of the fluorescence intensity on HOCl concentration (0.1–1.0 mM), stability in the physiological pH range, good selectivity, and high reaction rate with HOCl (fluorescence intensity plateau is reached within 3 s). Compound (**VI**) was used to visualize

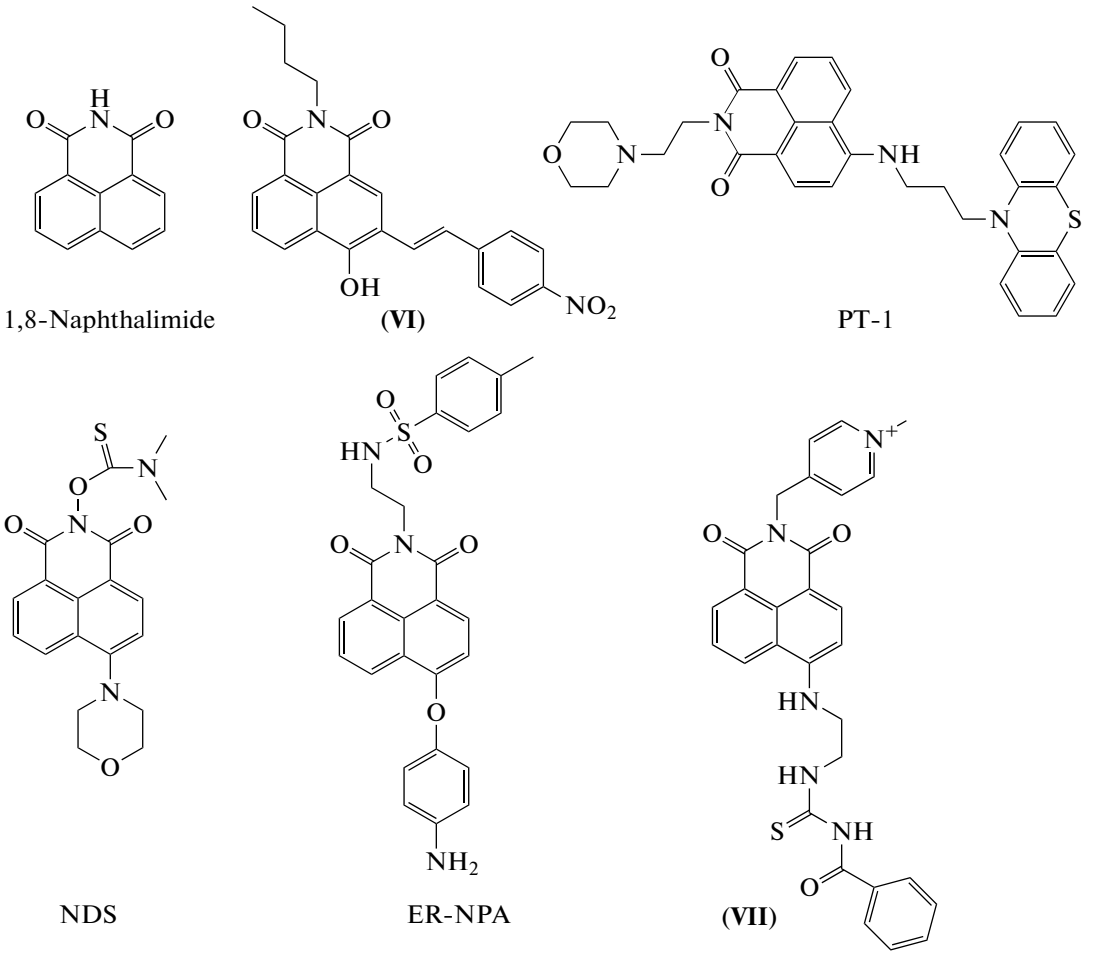

Fig. 11. Structural formulas of 1,8-naphthalimide and new fluorescent probes based thereon.

exogenous HOCl in A549 cells using confocal microscopy [80].

Also in 2017, Liu and coauthors presented a lysosome-targeted turn-on chemosensor PT-1 (Fig. 11) [81]. 1,8-Naphthalimide acts as a fluorophore, the phenothiazine moiety acts as an electron donor, and the morpholine moiety acts as a lysosomal targeting group. As a result of the reaction of HOCl with the sulfur atom in the phenothiazine fragment, the PET process is blocked, which increases the fluorescence intensity of the probe (λ_{ex} = 460 nm; λ_{em} = 535 nm). The probe has high values of such parameters as selectivity, sensitivity (LOD 0.88 nM), and quantum yield (0.57), as well as fast response (fluorescence intensity plateau is reached within 10 s); the operating pH range corresponds to the acidic region, which is necessary for registration of HOCl in lysosomes (pH 2–6). PT-1 was tested by detecting exogenous HOCl in L929 cells (murine cell line of subcutaneous connective tissue), as well as endogenous HOCl in RAW264.7 cells upon stimulation with LPS/PMA [81].

At the beginning of 2020, Jiao and coauthors presented the NDS turn-on chemosensor for HOCl detection (Fig. 11) [82]. In NDS, naphthalimide acts as a fluorophore, dimethylthiocarbamate acts as the HOCl reaction site, and the morpholine fragment ensures the penetration of the probe into lysosomes. It is assumed that HOCl reacts with the sulfur atom of the sensor, followed by hydrolysis of the target group. The buildup of the probe fluorescence intensity (λ_{ex} = 420 nm; λ_{em} = 525 nm) occurs due to the ICT process. NDS has a high sensitivity (LOD 105 nM), selectivity, and reaction rate with HOCl: the fluorescence intensity plateau is reached within 16 s when NDS reacts with HOCl in solution and within 300 s when reacting with HOCl formed in the $MPO/H_2O_2/Cl^-$ system. NDS was used to detect the formation of HOCl in lysosomes of HeLa cells upon their stimulation with LPS/PMA [82].

Also in 2020, another group of scientists led by Yang developed a probe of the turn-on type ER-NPA for registration of HOCl in endoplasmic reticulum (Fig. 11) [83]. Naphthalimide was used as a fluorophore, *p*-aminophenyl ether, as the HOCl reaction site; and methylsulfonamide, as a targeting group for the endoplasmic reticulum. It is assumed that in the

ER-NPA probe PET provides fluorescence quenching of naphthalimide, while in the presence of HOCl, oxidation and hydrolysis of the ester bond leads to the elimination of the aminophenyl residue and the formation of a hydroxyl anion, which promotes the ICT process and fluorescence buildup (λ_{ex} = 450 nm; λ_{em} = 550 nm). The probe showed high sensitivity (LOD 6.2 nM) and selectivity, as well as stability and a high level of fluorescence intensity under the action of HOCl in the pH range of 2–10. In the reaction with HOCl, a plateau in the fluorescence intensity is reached within 60 s. ER-NPA was used to detect exogenous and endogenous HOCl (upon stimulation with LPS/PMA, as well as with tunicamycin) in HeLa cells by confocal microscopy in the two-photon excitation mode (λ_{ex} = 800 nm; λ_{em} = 550 nm). This probe was also effective in detecting exogenous and endogenous HOCl (during stimulation with LPS/PMA) in vivo in embryos of aquarium fish *Danio rerio* [83].

In early 2021, Xu and coauthors presented a mitochondria-targeted probe of the turn-on type, compound (**VII**) [84]. The naphthalimide residue was used as a fluorophore, (2-aminoethyl)-thiourea was used as the reaction site, and the quaternized pyridine fragment was used as a mitochondria-targeting group. Interaction with HOCl results in intramolecular cyclization of the thiourea group of the probe, which is accompanied by an increase in fluorescence intensity (λ_{ex} = 370 nm; λ_{em} = 488 nm). The probe is characterized by selectivity to HOCl compared to other active forms, relatively high sensitivity (LOD 230 nM), and large operating pH range (pH 2–9); fluorescence intensity reaches a plateau within 60 s. The chemosensor was used to visualize exogenous HOCl in mitochondria of PC-12 cell line (cells of rat pheochromocytoma), as well as for recording the formation of endogenous HOCl in RAW264.7 cells upon their stimulation with PMA [84].

None of the probes listed in this subsection are commercially available.

Other Small-Molecule Probes

In 2016, a group of scientists led by Liu presented a hybrid turn-on probe based on the BODIPY and rhodamine cores, BRT (Fig. 12) [85]. In contrast to the precursors, for example, HRS1 and compound (**IV**) (Fig. 6), the oxygen atom in the rhodamine ring is replaced by a sulfur atom. Under the action of HOCl, rhodamine thiohydrazide transforms into the open form, which is accompanied by energy transfer via the FRET mechanism from the BODIPY core to rhodamine (λ_{ex} = 525 nm; λ_{em} = 580/540 nm). The probe showed high sensitivity (LOD 38 nM), selectivity, and reaction rate (the kinetic curve of fluorescence intensity reached a plateau within 15 s) with respect to HOCl compared to other oxidizing agents. However, buildup of the probe fluorescence intensity strongly depends on pH (optimum at pH 4.0–5.5). BRT was used to register HOCl production by RAW264.7 cells upon their activation by LPS by confocal microscopy [85].

In 2018, a group led by Song synthesized a new RPM switch probe (Fig. 12) [86]. In the structure of the chemosensor, imidazo[1,5-*a*]pyridine was used as an energy donor, and a modified rhodamine residue was used as an acceptor. The probe has its own fluorescence characteristic of imidazo[1,5-*a*]pyridine (λ_{ex} = 400 nm; λ_{em} = 462 nm). Upon reaction with HOCl, the carboxide group in imidazo[1,5-*a*]pyridine is converted to oxadiazole, which weakens its ability to accept electrons. On the other hand, the ring of the rhodamine fragment opens, which ultimately leads to an increase in the fluorescence intensity in the orange region of the spectrum while maintaining fluorescence in the blue region (λ_{ex} = 400 nm; λ_{em} = 587/462 nm). The authors believe that this effect is due to the combination of ICT and TBET. RPM has a high selectivity with respect to HOCl, a fast response (a plateau in the fluorescence intensity is reached within 30 s), and a large operating pH range (5.5–8.0), within which the efficiency of fluorescence switching is maximum and constant. The disadvantage of the sensor is its relatively low sensitivity (LOD 2.08 μM). RPM was used to visualize the production of HOCl by RAW264.7 cells upon stimulation with LPS by confocal microscopy [86].

Using the approach described above, in 2019, Meng and coauthors designed a CR-Ly ratiometric probe (Fig. 12) [87]. The coumarin and rhodamine cores were chosen as the energy donor and acceptor, respectively, and the morpholine fragment was chosen as the lysosome-targeted group. The switching of CR-Ly and compound (**IV**) described in the subsection on the transition to the concept of switching probes (Fig. 6) are similar. Diacylhydrazine acts as the HOCl reaction site, after interaction with which the rhodamine fragment undergoes a transformation from the spirocyclic form to the open-ring form. In this case, the unblocking of the FRET process leads to the switching of fluorescence from coumarin to rhodamine (λ_{ex} = 420 nm; λ_{em} = 582/479 nm). CR-Ly is characterized by extremely high sensitivity (LOD 12 nM) and selectivity with respect to HOCl, a relatively short reaction time (fluorescence intensity plateau is reached within 50 s). The ratio of changes in fluorescence intensity is the maximum and almost pH-independent in the weakly acidic region (pH 4–6), which corresponds to the goals of developing a probe for use in lysosomes. The possibility of visualizing HOCl production in lysosomes was shown in RAW264.7 cells stimulated with LPS/PMA [87].

In 2018, Zheng and coauthors presented the Dcp-EPtz turn-on probe based on phenothiazine-dicyanoisophorone (Fig. 12) [88]. Oxidation of the sulfur atom under the action of HOCl leads to the formation of aldehyde as a reaction product, which is characterized by fluorescence intensity in the red region (λ_{ex} =

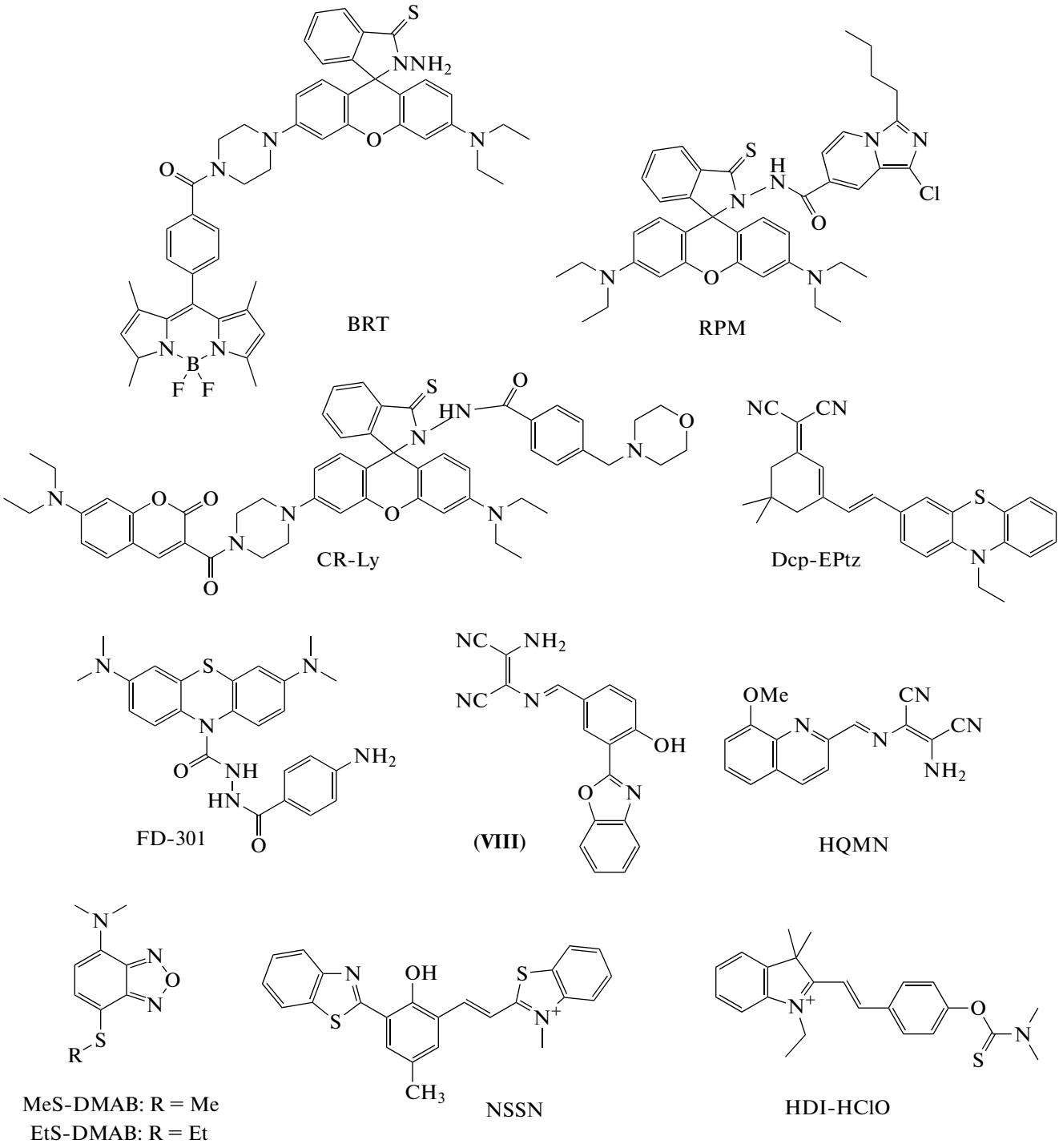

Fig. 12. Structural formulas of other new small-molecule fluorescent probes.

475 nm; λ_{em} = 618 nm) and a large Stokes shift (>143 nm). Dcp-EPtz has a high selectivity for HOCl compared to other oxidizing agents and a wide operating pH range of 5–8. However, due to the formation of radical intermediates, the fluorescence intensity of the reaction product is unstable during the first 300 s after the start of the reaction. Dcp-EPtz was used to detect exogenous HOCl in L929 cells by confocal microscopy and to produce endogenous HOCl in RAW264.7 cells upon their activation by LPS/PMA [88].

In mid-2020, Liu and coauthors developed and implemented a new approach to recording basal MPO activity [89]. The basis of the chemosensor of a turn-on type FD-301 (Fig. 12) is the structure of a well-

known MPO inhibitor, 4-aminobenzoic acid hydrazide, linked via a dibenzoylhydrazine linker to a fluorophore, methylene blue. FD-301 specifically binds to MPO via the hydrazide moiety, but steric hindrances caused by the presence of methylene blue does not lead to inhibition of the catalytic activity of the enzyme. The target of the reaction is a hydrazide residue, the oxidation of which with HOCl leads to the bond cleavage and fluorophore release (λ_{ex} = 620 nm; λ_{em} = 686 nm). FD-301 has a high sensitivity (LOD 44 nM) and rate of reaction with HOCl (fluorescence intensity plateau is reached in 10 s), a wide operating pH range of 3–8, and selectivity for HOCl compared to other oxidizing agents. The chemosensor was successfully tested for visualization of exogenous HOCl in RAW264.7 cells, as well as spontaneous production of endogenous HOCl in HL-60 cells. FD-301 was used to detect HOCl production in vivo in a model of arthritis induced by injection of λ-carrageenan into the mouse ankle joint and ex vivo in a model of murine ulcerative colitis induced by oral administration of 5% dextran [89].

In 2018, Chen and coauthors proposed a turn-on type probe (compound (**VIII**)) for the detection of HOCl based on the fluorescent core of 2-(2'-hydroxyphenyl)benzoxazole (Fig. 12) [90]. DAMN was chosen as the HOCl reaction site. When HOCl reacts with the probe, the imino group is converted into an aldehyde group. The reaction is accompanied by an increase in fluorescence intensity (λ_{ex} = 360 nm; λ_{em} = 435 nm) due to PET inhibition. The probe is characterized by high sensitivity, selectivity, and reaction rate (fluorescence intensity plateau is reached within 30 s) with respect to HOCl. The chemosensor was used in the two-photon excitation mode (λ_{ex} 740 nm) to detect the formation of HOCl in RAW264.7 cells upon their stimulation with LPS/IFN-γ/PMA, as well as in sections of the mouse hippocampus upon PMA stimulation [90].

In 2018, a group of scientists led by Das proposed a switch probe based on quinoline, HQMN (Fig. 12) [91]. Similar to compound (**VIII**), DAMN serves as the HOCl reaction site. The aldehyde obtained during the reaction of the probe with HOCl is characterized by a significant blue shift of the maximum fluorescence intensity (λ_{ex} = 370 nm; λ_{em} = 468/572 nm). The probe showed high selectivity with respect to HOCl compared to other oxidizing agents, as well as a large shift in the emission maximum under the action of HOCl (104 nm). However, the theoretical detection limit for HOCl (LOD 787 nM) is ~10 times greater than for many sensors developed in recent years, and the fluorescence intensity plateau is reached within 100 s, which is ~3 times greater than for probes of the phenoxazine series, probes based on rhodol, etc. Using HQMN, an increase in spontaneous production of HOCl in monocytes of diabetic patients compared with monocytes of healthy donors was registered [91].

In 2018, Sun and coauthors proposed two fluorescent probes of the turn-on type with benzofurazan as a fluorophore, MeS-DMAB and EtS-DMAB (Fig. 12) [92]. The thioether group is oxidized by the action of HOCl to a sulfoxide or sulfone group for MeS-DMAB and EtS-DMAB, respectively, which leads to an increase in the intensity of the fluorescence signal due to the activation of the ICT process (λ_{ex} = 440 nm; λ_{em} = 610 nm). Both chemosensors are characterized by a large Stokes shift (170 nm) and high selectivity for HOCl; however, the time it takes for the fluorescence intensity to reach a plateau after the addition of HOCl is 30–40 min. Since the sensitivity of EtS-DMAB (LOD 340 nM) to HOCl is higher compared to MeS-DMAB, it was used to detect exogenous HOCl in HeLa cells by confocal microscopy and to form endogenous HOCl in RAW264.7 cells upon their activation by LPS/IFN-γ/PMA [92].

In 2020, Huang and coauthors proposed a dual action probe NSSN for detecting HOCl in mitochondria (Fig. 12) [93]. The probe contains two benzothiazole fragments and one *p*-methylphenol residue between them. The reaction with HOCl proceeds via the C=C bond located between the *ortho*-position of *p*-methylphenol and benzothiazole, followed by elimination of the benzothiazole fragment. In this case, there is a switching of the probe fluorescence intensity from the red to the yellow region of the spectrum (λ_{ex} = 450 nm; λ_{em} = 540/670 nm), presumably due to the ESIPT process. At a HOCl concentration of 30–70 μM, the fluorescence emission spectrum shifts to the red region, and NSSN can be used as a turn-on probe (λ_{ex} = 450 nm; λ_{em} = 552 nm). The chemosensor is selective with respect to HOCl, has a low detection limit (LOD 130 nM), the operating range lies in the pH range of 7–10, but the fluorescence intensity plateau is reached within 5 min. NSSN was used to visualize exogenous HOCl in mitochondria of HeLa cells, as well as upon subcutaneous injection of HOCl into mice [93].

In 2021, Luo, together with Zhao, presented an HDI-HClO turn-on probe (Fig. 12) [94]. The probe contains fragments of indolenine, phenol, and, as in some other works, *N*,*N*-dimethylthiocarbamate as the HOCl reaction site. When the chemosensor reacts with HOCl, the previously blocked ICT process is activated, which leads to the fluorescence buildup (λ_{ex} = 440 nm; λ_{em} = 520 nm). HDI-HClO demonstrated high selectivity, high sensitivity (LOD 8.3 nM), rapid plateauing of the fluorescence intensity kinetic curve (8 s), and a wide operating pH range of 7–10. At the same time, the insignificant effect of biological thiols on the probe fluorescence intensity in the mode of kinetic studies should be noted. HDI-HClO was tested for visualization of exogenous HOCl in HeLa

cells, as well as endogenous HOCl in RAW264.7 macrophages upon their stimulation with LPS/PMA [94].

None of the probes listed in this subsection are commercially available.

A brief description of new small-molecule fluorescent probes for detecting HOCl is given in Table S1 (see Supplementary Information).

CONCLUSIONS

The development of sensitive, selective, and biologically compatible fluorescent probes for the detection of reactive compounds, including HOCl, in biological objects is of interest to many scientists; this has become particularly noticeable in the last 10 years. During this time, many probes have been developed based on various fluorescent cores, recognition groups, types, and ways of changing the fluorescence intensity. The probes themselves have become more specialized and more commonly used to monitor HOCl formation in order to study its involvement in physiological and pathophysiological processes, as well as elucidate the role of this molecule in cell signaling.

In this review, we presented a classification, detection strategies, and advances in the development of fluorescent probes for the detection of HOCl in biological samples. Despite significant advances in this area, there are a number of limitations to the use of fluorescent probes, regardless of their type: (1) a small Stokes shift, which leads to loss of probe sensitivity due to absorption of the emitted light; (2) slower reaction rate of HOCl with the sensor compared to functional groups of biomolecules, which complicates kinetic studies of the functional response of cells to external stimuli; (3) complicated synthetic procedures and, as a result, commercial unavailability, high cost, or low purity of the products; (4) a small operating pH range and/or its shift to acidic or alkaline regions (except for the development of probes aimed at specific target cell organelles); (5) low stability of the probe itself (short storage time of the preparation) and/or photobleaching of the fluorescent product during observations; (6) the effect of HOCl and other ROS, RHS, and RNS on the reaction product of the probe with HOCl; (7) low selectivity (high degree of influence of other ROS, RHS, and RNS, as well as ions); and (8) low sensitivity (high detection limit), etc. [16].

At present, a number of probes have been obtained devoid of most of the above disadvantages when used in cell-free media. However, this fact does not guarantee sufficient sensitivity of the same probe in cell cultures.

Taking into account the specifics of cellular systems, some additional requirements are imposed on probes for detecting HOCl.

(1) Ideally, the sensor should allow for selective assessment of HOCl production in intra- or extracellular areas. Therefore, when designing a probe, a balance between the hydrophobicity and hydrophilicity of the probe, appropriate for a particular task, in the context of membrane permeability, retention in cells, and solubility in physiological media should be observed [14].

(2) The ideal sensor solvent is water or physiological pH buffer. In some cases, small additions of an organic cosolvent are allowed. A high content of organic solvents can disrupt the physicochemical properties of biomolecules and affect cell viability. However, most fluorescent probes are poorly soluble in aqueous media. Organic substances such as *N*,*N*-dimethylformamide, dimethyl sulfoxide, acetonitrile, ethanol, and glycerol are used as solvents or cosolvents [95]. It should be kept in mind that the frequently used dimethyl sulfoxide is itself oxidized by HOCl [96]. Phosphate buffered saline, *N*-2-hydroxyethylpiperazine-*N*'-2-ethanesulfonic acid (HEPES), 2-amino-2-hydroxymethylpropane-1,3-diol (Tris), etc. are most often used as buffer solutions [95]. However, the use of the latter two compounds is undesirable due to their reaction with HOCl [97].

(3) It is necessary to avoid strong absorption of the probe in the ultraviolet region, as well as the overlap of the absorption and/or excitation spectra of the sensor with the Soret bands of the main proteins of blood plasma. The first of these problems can be circumvented by using the two-photon excitation mode of the chemosensor, which, however, is not always realizable.

(4) The probe must be nontoxic to cells at the concentrations used throughout the entire measurement period (depending on the methods used, the time interval varies from 30 min to several days). In this case, it is desirable that the probe has a high molar absorption coefficient, which makes it possible to reduce its concentration required for experiments and, consequently, to reduce interference in the mechanisms under study [14].

When developing a probe devoid of several shortcomings at once, researchers often take some successful solution as a basis in order to further refine it. Thus, among the trends in the development and application of small-molecule probes for detecting HOCl, one can note the frequent use of DAMN as a target for HOCl in sensors, for example, in CSN [63], RO610 [78], compound (**VIII**) [90], and HQMN [91]. A new branch was the use of probes based on phenoxazine (CB [70], RT-1 [73], BR-O [74], BR-1 [75], BC-2, and BC-3 [77]), as well as a hybrid fluorophore rhodol (RO610 [78], HKOCl-4, and its derivatives [79]). Of interest is the strategy of simultaneous registration of several types of oxidants, implemented, for example, in the work of Zhang et al. [67] using the FHZ probe as an example.

Growing complication of the structure of probes is observed due to the introduction of additional targets to increase the selectivity and/or sensitivity of sensors, as well as the more frequent use of donor–acceptor

pairs to create probes of the switch type. The general trend is the development of probes with a large Stokes shift and registration in the near infrared range (alternatively, probes with the possibility of two-photon excitation) compatible with commonly used laser wavelengths (for example, 488, 640, 750 nm, etc.) [32, 33].

Of the new small-molecule probes presented in this review (Table S1 in Supplementary Information), depending on the objectives of the study and based on the data indicated by the authors of the articles, the following probes are suitable for detecting HOCl:

(1) According to the HOCl registration method used:

(a) For confocal microscopy, all of the indicated probes.

(b) For flow cytometry, HKOCl-3 [64], CB [70–72], and HKOCl-4r [79].

(c) For research in cell suspensions using a spectrofluorometer, HKOCl-3 [64], CB [70–72].

(d) For kinetic studies of HOCl formation (reaction time <1 min), all probes other than BCO and BETC (reaction time not determined) [62], FN-1 and FN-2 [69], RT-1 [73], BR-O [74], BR-1 [75], Dcp-EPtz [88], EtS-DMAB [92], NSSN [93].

(2) For registration of HOCl production in cell organelles:

(a) In mitochondria, FHZ (in cytoplasm and mitochondria) [67], HKOCl-4m [79], and compound (**VII**) [84], NSSN [93].

(b) In lysosomes, NDS [82], CR-Ly [87].

(c) In the endoplasmic reticulum, ER-NPA [83].

(3) To register the formation of HOCl:

(a) In vivo, FHZ [67], BR-1 [75], BC-3 [77], RO610 [78], ER-NPA [83], FD-301 [89], NSSN [93].

(b) In tissue sections, HKOCl-4r [79], compound (**VIII**) [90].

(4) Using near infrared or two-photon excitation mode:

(a) CSN, switching from the red region of the spectrum to the blue (λ_{em} = 470/640 nm) [63]; NSSN, switching from the red region of the spectrum to the yellow region (λ_{em} = 540/670 nm) [93].

(b) Excitation and emission in the red region of the spectrum, BR-O [74], BR-1 [75], and BC-3 [77] (λ_{ex} = 610 nm; λ_{em} = 670 nm), FD-301 (λ_{ex} = 620 nm; λ_{em} = 686 nm) [89].

(c) BRT switching from the blue region of the spectrum to orange while maintaining the red band (λ_{em} 587/462 nm) [85].

(d) The possibility of using two-photon excitation, compound (**VIII**) (λ_{ex} = 740 nm; λ_{em} = 435 nm) [90], ER-NPA (λ_{ex} = 800 nm; λ_{em} = 550 nm) [83].

The following probes are currently commercially available for purchase: HKOCl-3 (CAS 2031170-80-4), FHZ (CAS 1883737-63-0), CB (CAS 1562-90-9), HKOCl-4 (CAS 2031170-85-9), and HKOCl-4m (CAS 2031170-88-2).

In 2016–2021, undoubted progress has been made in the development of small-molecule fluorescent probes, as well as their application for visualization of HOCl both in vitro and in vivo. However, many problems associated with the sensitivity and selectivity of probes, the rate of their reaction with HOCl (for kinetic studies), low Stokes shift, the use of organic solvents, and low photostability remain topical even now. In this regard, when choosing a chemosensor for practical use, it is necessary to pay attention to the set of probe characteristics that will allow solving the specific problem set for the experimenter in the most efficient manner. In addition, a very small number of developed chemosensors are available for direct purchase, which causes additional difficulties for researchers, but at the same time opens up the possibility and need for further design and synthesis of new probes for detecting HOCl.

FUNDING

This work was financially supported by the Belarusian Republican Foundation for Basic Research (project no. B20R-215), the Russian Foundation for Basic Research (project no. 20-515-00006), and grant no. MD1901.2020.4 from the President of the Russian Federation.

The description of the phenoxazine-based probes, as well as some others, was supported by the Russian Science Foundation (project no. 20-15-00390), for which their use is planned.

COMPLIANCE WITH ETHICAL STANDARDS

This article does not contain any research involving humans or animals as research objects.

Conflict of Interests

The authors declare no conflicts of interest.

SUPPLEMENTARY INFORMATION

The online version contains supplementary material available at https://doi.org/10.1134/S1068162022030165.

REFERENCES

1. Alfadda, A.A. and Sallam, R.M., *J. Biomed. Biotechnol.*, 2012, vol. 2012, pp. 936486–936499. https://doi.org/10.1155/2012/936486
2. Milkovic, L., Cipak Gasparovic, A., Cindric, M., Mouthuy, P.A., and Zarkovic, N., *Cells*, 2019, vol. 8, pp. 793–806. https://doi.org/10.3390/cells8080793
3. Phaniendra, A., Jestadi, D.B., and Periyasamy, L., *Indian J. Clin. Biochem.*, 2015, vol. 30, pp. 11–26. https://doi.org/10.1007/s12291-014-0446-0

4. Winterbourn, C.C., *Toxicology*, 2002, vol. 181, pp. 223–227. https://doi.org/10.1016/S0300-483X(02)00286-X
5. Arnhold, J., *Int. J. Mol. Sci.,* 2020, vol. 21, pp. 8057–8084. https://doi.org/10.3390/ijms21218057
6. Panasenko, O.M., Gorudko, I.V., and Sokolov, A.V., *Biochemistry (Moscow)*, 2013, vol. 78, pp. 1466–1489. https://doi.org/10.1134/S0006297913130075
7. Ulfig, A. and Leichert, L.I., *Cell. Mol. Life Sci.*, 2021, vol. 78, pp. 385–414. https://doi.org/10.1007/s00018-020-03591-y
8. Pattison, D.I. and Davies, M.J., *Chem. Res. Toxicol.*, 2001, vol. 14, pp. 1453–1464. https://doi.org/10.1021/tx0155451
9. Zhang, L., Wang, X., Cueto, R., Effi, C., Zhang, Y., Tan, H., Qin, X., Ji, Y., Yang, X., and Wang, H., *Redox Biol.*, 2019, vol. 26, pp. 101284–101299. https://doi.org/10.1016/j.redox.2019.101284
10. Chen, X., Tian, X., Shin, I., and Yoon, J., *Chem. Soc. Rev.*, 2011, vol. 40, pp. 4783–4804. https://doi.org/10.1039/C1CS15037E
11. Burns, J.M., Cooper, W.J., Ferry, J.L., King, D.W., DiMento, B.P., McNeill, K., Miller, C.J., Miller, W.L., Peake, B.M., Rusak, S.A., Rose, A.L., and Waite, T.D., *Aquat. Sci.*, 2012, vol. 74, pp. 683–734. https://doi.org/10.1007/s00027-012-0251-x
12. Hu, J.J., Ye, S., and Yang, D., *Isr. J. Chem.*, 2017, vol. 57, pp. 251–258. https://doi.org/10.1002/ijch.201600113
13. Yudhistira, T., Mulay, S.V., Kim, Y., Halle, M.B., and Churchill, D.G., *Chem. Asian J.*, 2019, vol. 14, pp. 3048–3084. https://doi.org/10.1002/asia.201900672
14. Chan, J., Dodani, S.C., and Chang, C.J., *Nat. Chem.*, 2012, vol. 4, pp. 973–984. https://doi.org/10.1038/nchem.1500
15. Dong, S., Zhang, L., Lin, Y., Ding, C., and Lu, C., *Analyst*, 2020, vol. 145, pp. 5068–5089. https://doi.org/10.1039/D0AN00645A
16. Zhang, R., Song, B., and Yuan, J., *TrAC Trends Anal. Chem.*, 2018, vol. 99, pp. 1–33. https://doi.org/10.1016/j.trac.2017.11.015
17. Wan, J., Zhang, X., Zhang, K., and Su, Z., *Rev. Anal. Chem.*, 2020, vol. 39, pp. 209–221. https://doi.org/10.1515/revac-2020-0119
18. Tholen, D.W., Linnet, K., Kondratovich, M., Armbruster, D.A., Garrett, P.E., Jones, R.L., Kroll, M.H., Lequin, R.M., Pankratz, T.J., Scassellati, G.A., Schimmel, H., and Tsai, J., *Clinical and Laboratory Standards Institute (CLSI). Protocols for Determination of Limits of Detection and Limits of Quantitation, Approved Guideline*, CLSI document EP17-A.CLSI, Wayne, PA, 2004. https://demo.nextlab.ir/Organization/Documents/CLSI-Standards/CLSI-EP17-A.aspx.
19. Long, G.L. and Winefordner, J.D., *Anal. Chem. Am. Chem. Soc.*, 1983, vol. 55, p. 712A–724A. https://doi.org/10.1021/ac00258a001
20. Ruff, F., Szabo, D., Rabai, J., Jalsovszky, I., and Farkas, O., *J. Phys. Org. Chem.*, 2019, vol. 32, art. ID e4005. https://doi.org/10.1002/poc.4005
21. Lin, W., Long, L., Chen, B., and Tan, W., *Chemistry*, 2009, vol. 15, pp. 2305–2309. https://doi.org/10.1002/chem.200802054
22. Yue, Y., Huo, F., Yin, C., Escobedo, J.O., and Strongin, R.M., *Analyst*, 2016, vol. 141, pp. 1859–1873. https://doi.org/10.1039/C6AN00158K
23. Bai, X., Ng, K.K.H., Hu, J.J., Ye, S., and Yang, D., *Annu. Rev. Biochem.*, 2019, vol. 88, pp. 605–633. https://doi.org/10.1146/annurev-biochem-013118-111754
24. Bartosz, G., *Clin. Chim. Acta*, 2006, vol. 368, pp. 53–76. https://doi.org/10.1016/j.cca.2005.12.039
25. Zhang, Y.R., Liu, Y., Feng, X., and Zhao, B.X., *Sens. Actuators*, 2017, vol. 240, pp. 18–36. https://doi.org/10.1016/j.snb.2016.08.066
26. Winterbourn, C.C., *Biochim. Biophys. Acta*, 2014, vol. 1840, pp. 730–738. https://doi.org/10.1016/j.bbagen.2013.05.004
27. Gao, P., Pan, W., Li, N., and Tang, B., *Chem. Sci.*, 2019, vol. 10, pp. 6035–6071. https://doi.org/10.1039/C9SC01652J
28. Fu, Y. and Finney, N.S., *RSC Adv.*, 2018, vol. 8, pp. 29051–29061. https://doi.org/10.1039/C8RA02297F
29. Cao, D., Zhu, L., Liu, Z., and Lin, W., *J. Photochem. Photobiol. C Photochem. Rev.*, 2020, vol. 44, art. ID 100371. https://doi.org/10.1016/j.jphotochemrev.2020.100371
30. Jiao, Y., Zhu, B., Chen, J., and Duan, X., *Theranostics*, 2015, vol. 5, pp. 173–187. https://doi.org/10.7150/thno.9860
31. Yuan, L., Lin, W., Xie, Y., Chen, B., and Song, J., *Chemistry*, 2012, vol. 18, pp. 2700–2706. https://doi.org/10.1002/chem.201101918
32. Wang, L., Du, W., Hu, Z., Uvdal, K., Li, L., and Huang, W., *Angew. Chem., Int. Ed. Engl.,* 2019, vol. 58, pp. 14026–14043. https://doi.org/10.1002/anie.201901061
33. Andina, D., Leroux, J.C., and Luciani, P., *Chemistry*, 2017, vol. 23, pp. 13549–13573. https://doi.org/10.1002/chem.201702458
34. Cao, D., Liu, Z., Verwilst, P., Koo, S., Jangili, P., Kim, J.S., and Lin, W., *Chem. Rev.*, 2019, vol. 119, pp. 10403–10519. https://doi.org/10.1021/acs.chemrev.9b00145
35. Kenmoku, S., Urano, Y., Kojima, H., and Nagano, T., *J. Am. Chem. Soc.*, 2007, vol. 129, pp. 7313–7318. https://doi.org/10.1021/ja068740g
36. Koide, Y., Urano, Y., Hanaoka, K., Terai, T., and Nagano, T., *J. Am. Chem. Soc.*, 2011, vol. 133, pp. 5680–5682. https://doi.org/10.1021/ja111470n
37. Chen, X., Lee, K.A., Ha, E.M., Lee, K.M., Seo, Y.Y., Choi, H.K., Kim, H.N., Kim, M.J., Cho, C.S., Lee, S.Y., Lee, W.J., and Yoon, J., *Chem. Commun.*, 2011, vol. 47, pp. 4373–4375. https://doi.org/10.1039/C1CC10589B

38. Zhou, J., Li, L., Shi, W., Gao, X., Li, X., and Ma, H., *Chem. Sci.*, 2015, vol. 6, pp. 4884–4888. https://doi.org/10.1039/C5SC01562F
39. Bruno, J.G., Herman, T.S., Cano, V.L., Stribling, L., and Kiel, J.L., *In Vitro Cell. Dev. Biol. Anim.*, 1999, vol. 35, pp. 376–382. https://doi.org/10.1007/s11626-999-0111-8
40. Adachi, Y., Kindzelskii, A.L., Petty, A.R., Huang, J.B., Maeda, N., Yotsumoto, S., Aratani, Y., Ohno, N., and Petty, H.R., *J. Immunol.*, 2006, vol. 176, pp. 5033–5040. https://doi.org/10.4049/jimmunol.176.8.5033
41. Yang, Y.K., Cho, H.J., Lee, J., Shin, I., and Tae, J., *Org. Lett.*, 2009, vol. 11, pp. 859–861. https://doi.org/10.1021/ol802822t
42. Zhang, Z., Zheng, Y., Hang, W., Yan, X., and Zhao, Y., *Talanta*, 2011, vol. 85, pp. 779–786. https://doi.org/10.1016/j.talanta.2011.04.078
43. Zhang, Z., Deng, C., Meng, L., Zheng, Y., and Yan, X., *Anal. Methods*, 2015, vol. 7, pp. 107–114. https://doi.org/10.1039/C4AY02281E
44. Setsukinai, K.I., Urano, Y., Kakinuma, K., Majima, H.J., and Nagano, T., *J. Biol. Chem.*, 2003, vol. 278, pp. 3170–3175. https://doi.org/10.1074/jbc.M209264200
45. Cohn, C.A., Pedigo, C.E., Hylton, S.N., Simon, S.R., and Schoonen, M.A., *Geochem. Trans.*, 2009, vol. 10, pp. 1–9. https://doi.org/10.1186/1467-4866-10-8
46. Flemmig, J., Zschaler, J., Remmler, J., and Arnhold, J., *J. Biol. Chem.*, 2012, vol. 287, pp. 27913–27923. https://doi.org/10.1074/jbc.M112.364299
47. Flemmig, J., Schwarz, P., Bäcker, I., Leichsenring, A., Lange, F., and Arnhold, J., *J. Immunol. Methods*, 2014, vol. 415, pp. 46–56. https://doi.org/10.1016/j.jim.2014.09.003
48. Shepherd, J., Hilderbrand, S.A., Waterman, P., Heinecke, J.W., Weissleder, R., and Libby, P., *Chem. Biol.*, 2007, vol. 14, pp. 1221–1231. https://doi.org/10.1016/j.chembiol.2007.10.005
49. Xu, Q., Lee, K.A., Lee, S., Lee, K.M., Lee, W.J., and Yoon, J., *J. Am. Chem. Soc.*, 2013, vol. 135, pp. 9944–9949. https://doi.org/10.1021/ja404649m
50. Sun, Z.N., Liu, F.Q., Chen, Y., Tam, P.K.H., and Yang, D., *Org. Lett.*, 2008, vol. 10, pp. 2171–2174. https://doi.org/10.1021/ol800507m
51. Yang, D., Sun, Z.N., Peng, T., Wang, H.L., Shen, J.G., Chen, Y., and Tam, P.K.H., in *Live Cell Imaging*, Papkovsky, D., Ed., Humana Press, 2010, vol. 591, pp. 93–103. https://doi.org/10.1007/978-1-60761-404-3
52. Hu, J.J., Wong, N.K., Gu, Q., Bai, X., Ye, S., and Yang, D., *Org. Lett.*, 2014, vol. 16, pp. 3544–3547. https://doi.org/10.1021/ol501496n
53. Murao, S.L., Stevens, F.J., Ito, A., and Huberman, E., *Proc. Natl. Acad. Sci. U. S. A.*, 1988, vol. 85, pp. 1232–1236. https://doi.org/10.1073/pnas.85.4.1232
54. Gai, L., Mack, J., Liu, H., Xu, Z., Lu, H., and Li, Z., *Sens. Actuators*, 2013, vol. 182, pp. 1–6. https://doi.org/10.1016/j.snb.2013.02.106
55. Emrullahoğlu, M., Üçüncü, M., and Karakuş, E., *Chem. Commun.*, 2013, vol. 49, pp. 7836–7838. https://doi.org/10.1039/C3CC44463E
56. Liu, S.R. and Wu, S.P., *Org. Lett.*, 2013, vol. 15, pp. 878–881. https://doi.org/10.1021/ol400011u
57. Long, L., Zhang, D., Li, X., Zhang, J., Zhang, C., and Zhou, L., *Anal. Chim. Acta*, 2013, vol. 775, pp. 100–105. https://doi.org/10.1016/j.aca.2013.03.016
58. Zhang, Y.R., Chen, X.P., Zhang, J.Y., Yuan, Q., Miao, J.Y., and Zhao, B.X., *Chem. Commun.*, 2014, vol. 50, pp. 14241–14244. https://doi.org/10.1039/C4CC05976J
59. Wang, L., Long, L., Zhou, L., Wu, Y., Zhang, C., Han, Z., Wang, J., and Da, Z., *RSC Adv.*, 2014, vol. 4, pp. 59535–59540. https://doi.org/10.1039/C4RA10633D
60. Goswami, S., Aich, K., Das, S., Pakhira, B., Ghoshal, K., Quah, C.K., Bhattacharyya, M., Fun, H.K., and Sarkar, S., *Chem. Asian J.*, 2015, vol. 10, pp. 694–700. https://doi.org/10.1002/asia.201403234
61. Liu, Z., Li, G., Wang, Y., Li, J., Mi, Y., Guo, L., Xu, W., Zou, D., Li, T., and Wu, Y., *RSC Adv.*, 2018, vol. 8, pp. 9519–9523. https://doi.org/10.1039/C7RA13419C
62. Jin, L., Tan, X., Zhao, C., and Wang, Q., *Anal. Methods*, 2019, vol. 11, pp. 1916–1922. https://doi.org/10.1039/C9AY00105K
63. Shi, L., Yu, H., Zeng, X., Yang, S., Gong, S., Xiang, H., Zhang, K., and Shao, G., *New J. Chem.*, 2020, vol. 44, pp. 6232–6237. https://doi.org/10.1039/D0NJ00318B
64. Hu, J.J., Wong, N.K., Lu, M.Y., Chen, X., Ye, S., Zhao, A.Q., Gao, P., Kao, R.Y.-T., Shen, J., and Yang, D., *Chem. Sci.*, 2016, vol. 7, pp. 2094–2099. https://doi.org/10.1039/C5SC03855C
65. Chang, C.Y., Song, M.J., Jeon, S.B., Yoon, H.J., Lee, D.K., Kim, I.H., Suk, K., Choi, D.K., and Park, E.J., *Am. J. Pathol.*, 2011, vol. 179, pp. 964–979. https://doi.org/10.1016/j.ajpath.2011.04.033
66. Agrawal, I., Sharma, N., Saxena, S., Arvind, S., Chakraborty, D., Chakraborty, D.B., Jha, D., Ghatak, S., Epari, S., Gupta, T., and Jha, S., *iScience*, 2021, vol. 24, pp. 101968–101978. https://doi.org/10.1016/j.isci.2020.101968
67. Zhang, R., Zhao, J., Han, G., Liu, Z., Liu, C., Zhang, C., Liu, B., Jiang, C., Liu, R., Zhao, T., Han, M.Y., and Zhang, Z., *J. Am. Chem. Soc.*, 2016, vol. 138, pp. 3769–3778. https://doi.org/10.1021/jacs.5b12848
68. Zhou, Y., Wang, Y.K., Wang, X.F., Zhang, Y.J., and Wang, C.K., *Chin. Phys. B*, 2017, vol. 26, art. ID 083102-1–083102-7. https://doi.org/10.1088/1674-1056/26/8/083102
69. Lv, J., Wang, F., Wei, T., and Chen, X., *Ind. Eng. Chem. Res.*, 2017, vol. 56, pp. 3757–3764. https://doi.org/10.1021/acs.iecr.7b00381
70. Kozlov, S.O., Kudryavtsev, I.V., Grudinina, N.A., Kostevich, V.A., Panasenko, O.M., Sokolov, A.V., and Vasil'ev, V.B., *Acta Biomed. Sci.*, 2016, vol. 1, pp. 86–

91.
https://doi.org/10.12737/article_590823a4895537.04307905

71. Sokolov, A.V., Kostevich, V.A., Kozlov, S.O., Donskyi, I.S., Vlasova, I.I., Rudenko, A.O., Zakharova, E.T., Vasilyev, V.B., and Panasenko, O.M., *Free Radical Res.*, 2015, vol. 49, pp. 777–789. https://doi.org/10.3109/10715762.2015.1017478
72. Lutsenko, V.E., Grigorieva, D.V., Gorudko, I.V., Cherenkevich, S.N., Gorbunov, N.N., Kostevich, V.A., Panasenko, O.M., and Sokolov, A.V., *Med. Acad. J.*, 2019, vol. 19, pp. 63–71. https://doi.org/10.17816/MAJ19263-71
73. Choi, M.G., Lee, Y.J., Lee, K.M., Park, K.Y., Park, T.J., and Chang, S.K., *Analyst*, 2019, vol. 144, pp. 7263–7269. https://doi.org/10.1039/C9AN01884K
74. Yang, J., Yao, Y., Shen, Y., Xu, Y., Lv, G., and Li, C., *ZAA*, vol. 646, pp. 431–436. https://doi.org/10.1002/zaac.202000127
75. Yang, J., Zheng, W., Shen, Y., Xu, Y., Lv, G., and Li, C., *J. Lumin.*, 2020, vol. 226, pp. 117460–117466. https://doi.org/10.1016/j.jlumin.2020.117460
76. Hansra, P., Moran, E.L., Fornasier, V.L., and Bogoch, E.R., *Inflammation*, 2000, vol. 24, pp. 141–155. https://doi.org/10.1023/A:1007033610430
77. Zheng, W., Yang, J., Shen, Y., Yao, Y., Lv, G., Hao, S., and Li, C., *Dyes Pigm.*, 2020, vol. 179, pp. 108404–108410. https://doi.org/10.1016/j.dyepig.2020.108404
78. Zhang, Y., Ma, L., Tang, C., Pan, S., Shi, D., Wang, S., Li, M., and Guo, Y., *J. Mater. Chem.*, vol. 6, pp. 725–731. https://doi.org/10.1039/C7TB02862H
79. Bai, X., Yang, B., Chen, H., Shen, J., and Yang, D., *Org. Chem. Front.*, 2020, vol. 7, pp. 993–996. https://doi.org/10.1039/D0QO00081G
80. Li, J., Yin, C., Liu, T., Wen, Y., and Huo, F., *Sens. Actuators*, 2017, vol. 252, pp. 1112–1117. https://doi.org/10.1016/j.snb.2017.07.171
81. Liu, C., Jiao, X., He, S., Zhao, L., and Zeng, X., *Talanta*, 2017, vol. 174, pp. 234–242. https://doi.org/10.1016/j.talanta.2017.06.012
82. Jiao, C., Liu, Y., Pang, J., Lu, W., Zhang, P., and Wang, Y., *J. Photochem. Photobiol. Chem.*, 2020, vol. 392, pp. 112399–112405. https://doi.org/10.1016/j.jphotochem.2020.112399
83. Yang, T., Sun, J., Yao, W., and Gao, F., *Dyes Pigments*, 2020, vol. 180, pp. 108435–108442. https://doi.org/10.1016/j.dyepig.2020.108435
84. Xu, J., Wang, C., Ma, Q., Zhang, H., Tian, M., Sun, J., Wang, B., and Chen, Y., *ACS Omega*, 2021, vol. 6, pp. 14399–14409. https://doi.org/10.1021/acsomega.1c01271
85. Liu, Y., Zhao, Z.M., Miao, J.Y., and Zhao, B.X., *Anal. Chim. Acta*, 2016, vol. 921, pp. 77–83. https://doi.org/10.1016/j.aca.2016.03.045
86. Song, G.J., Ma, H.L., Luo, J., Cao, X.Q., and Zhao, B.X., *Dyes Pigments*, 2018, vol. 148, pp. 206–211. https://doi.org/10.1016/j.dyepig.2017.09.022
87. Meng, H., Huang, X.Q., Lin, Y., Yang, D.Y., Lv, Y.J., Cao, X.Q., Zhang, G.X., Dong, J., and Shen, S.L., *Spectrochim. Acta. A. Mol. Biomol. Spectrosc.*, 2019, vol. 223, pp. 117355–117360. https://doi.org/10.1016/j.saa.2019.117355
88. Zheng, D., Qiu, X., Liu, C., Jiao, X., He, S., Zhao, L., and Zeng, X., *New J. Chem.*, 2018, vol. 42, pp. 5135–5141. https://doi.org/10.1039/C8NJ00279G
89. Liu, L., Wei, P., Yuan, W., Liu, Z., Xue, F., Zhang, X., and Yi, T., *Anal. Chem.*, 2020, vol. 92, pp. 10971–10978. https://doi.org/10.1021/acs.analchem.9b04601
90. Chen, L., Park, S.J., Wu, D., Kim, H.M., and Yoon, J., *Dyes Pigments*, 2018, vol. 158, pp. 526–532. https://doi.org/10.1016/j.dyepig.2018.01.027
91. Das, S., Aich, K., Patra, L., Ghoshal, K., Gharami, S., Bhattacharyya, M., and Mondal, T.K., *Tetrahedron Lett.*, 2018, vol. 59, pp. 1130–1135. https://doi.org/10.1016/j.tetlet.2018.02.023
92. Sun, J., Zhang, L., Hu, Y., and Fang, J., *Sens. Actuators*, 2018, vol. 266, pp. 447–454. https://doi.org/10.1016/j.snb.2018.03.124
93. Huang, Y., Zhang, Y., Huo, F., Liu, Y., and Yin, C., *Dyes Pigments*, 2020, vol. 179, pp. 108387–108393. https://doi.org/10.1016/j.dyepig.2020.108387
94. Luo, P. and Zhao, X., *ACS Omega*, 2021, vol. 6, pp. 12287–12292. https://doi.org/10.1021/acsomega.1c01102
95. Wu, D., Chen, L., Xu, Q., Chen, X., and Yoon, J., *Acc. Chem. Res.*, 2019, vol. 52, pp. 2158–2168. https://doi.org/10.1021/acs.accounts.9b00307
96. Imaizumi, N., Kanayama, T., and Oikawa, K., *Analyst*, 1995, vol. 120, pp. 1983–1987. https://doi.org/10.1039/AN9952001983
97. Prütz, W.A., *Arch. Biochem. Biophys.*, 1996, vol. 332, pp. 110–120. https://doi.org/10.1006/abbi.1996.0322

Translated by N. Onishchenko